



FCTUC FACULDADE DE CIÊNCIAS
E TECNOLOGIA
UNIVERSIDADE DE COIMBRA

DEPARTAMENTO DE
ENGENHARIA MECÂNICA

Corte por jacto de água de compósitos de matriz polimérica com reforço de fibra de carbono

Cutting of carbon fiber reinforced polymer composites using abrasive water jet technology

Dissertação apresentada para a obtenção do grau de Mestre em Engenharia Mecânica na Especialidade de Sistemas de Produção

Autor

Hugo das Neves Costa Antunes

Coordenadores

Professor Doutor Altino de Jesus Roque Loureiro

Professor Doutor Peter Bjurstam

Júri

Presidente	Professora Doutora Marta Cristina Cardoso de Oliveira Professora Auxiliar da Universidade de Coimbra Professor Doutor Altino de Jesus Roque Loureiro Professor Associado com Agregação da Universidade de Coimbra Professora Doutora Dulce Maria Esteves Rodrigues
Vogais	Professora Auxiliar da Universidade de Coimbra Professora Doutora Cristina Maria Gonçalves dos Santos Louro Professora Auxiliar da Universidade de Coimbra



**Linköping University -
Sweden**

Coimbra - Portugal, Setembro, 2011

"Whenever you are asked if you can do a job, tell 'em, "Certainly I can!" then
get busy and find out how to do it."

Theodore Roosevelt

Acknowledgments / Agradecimentos

O trabalho aqui apresentado representa o termo de uma fase da minha vida, e como tal, não posso deixar de expressar o meu profundo agradecimento a todas as pessoas que me acompanharam, que pela sua dedicação, amizade e companheirismo tornaram este percurso mais fácil, possível e agradável. No entanto, devido ao papel fulcral de algumas pessoas, torna-se incontornável expressar um particular agradecimento:

Ao Exmo. Senhor Professor Altino de Jesus Roque Loureiro, *que mesmo impedido, por razões geográficas, de seguir o desenvolvimento do meu trabalho, sempre demonstrou uma infundável vontade de ajudar, tendo desempenhado um papel preponderante durante a escrita e revisão do mesmo.*

To all the Professors responsible for supervising my work at Linköping University, especially Professor Peter Bjurström and Professor Stefan Björklund, members of the Production Systems division, department of Management and Engineering, *for the way they embraced this challenge. Their understanding and encouraging have proved to be crucial for the development of this work.*

To all the staff of the machine shop of the Production Systems Division (LiU), especially Mr. Sören and Mr. Vitaly, *by their crucial assistance and willingness. Without them the experimental part of this work would be unachievable.*

A todos os docentes, funcionários e colegas do Departamento de Engenharia Mecânica, *pela excelência apresentada no desempenho das suas funções, que permitiu que considerasse o DEM como uma casa.*

A todos os meus Amigos, *sem os quais não teria sido possível concluir esta fase com sucesso, e com os quais conto partilhar outros momentos de alegria. Se poderia viver sem eles? Podia! Mas certamente não seria a mesma coisa...*

Ao meu colega e amigo Vinhaça, ao qual não poderia deixar de agradecer particularmente, por me ter acompanhado nesta aventura da qual guardo recordações únicas, certamente importantes e enriquecedoras para a minha vida futura.

Aos meus Primos, Diogo e Filipa, pela maneira como me receberam em sua casa, levando a que neste momento os considere como os “meus irmãos”.

Aos meus avós, Vovó Dála e Vovô Zé, pelo papel essencial que desempenharam na minha formação pessoal, com toda a paciência e carinho do mundo.

À Liliana, por me ter aturado todos estes anos, contribuindo para o meu sucesso pessoal e académico, dando apoio e carinho nos momentos cruciais. De notar também a imensa paciência que demonstrou nas maiores alturas de stress, principalmente próximo à entrega deste trabalho.

Aos meus Tios, Titi Zé e Tio Carlos, que me acolheram como um filho ao longo dos meus 7 anos de curso, com todos os benefícios de uma relação deste género, aos quais ficarei eternamente grato.

E por fim aos meus Pais, porque afinal de contas, é graças a eles que posso escrever estas mesmas linhas. Tenho também que agradecer pela liberdade que me deram para aprender com os meus próprios erros, dando ao mesmo tempo total apoio e confiança, com conselhos preciosos e repreensões acertadas. Modéstia à parte, os melhores pais do mundo

Resumo

Os materiais compósitos, apesar das manifestas vantagens, especialmente quando as aplicações em que se inserem exigem uma criteriosa selecção de materiais com um rácio resistência/peso o mais elevado possível, apresentam ainda custos elevados pelo que o seu uso é restringido a algumas aplicações.

Os compósitos de matriz polimérica com reforço de fibras de carbono, vulgarmente conhecidos por fibras de carbono, são materiais difíceis de maquinar por métodos tradicionais, pelo que o corte por jacto de água com abrasivos, devido à não geração de calor durante o processo, tem ganho relevância por evitar problemas, como, por exemplo, o desgaste excessivo das ferramentas e zonas termicamente afectadas nas peças. No entanto, o corte com recurso a esta tecnologia cria algumas características distintas nas paredes de corte, que podem ser consideradas como defeitos, dependendo da sua magnitude e da utilização posterior da peça cortada.

O presente estudo pretende analisar a influência da velocidade e da orientação de corte nestas características. Para tal foram executados cortes com diferentes velocidades e orientações, cortes estes que foram depois caracterizados quanto à rugosidade e inclinação das suas paredes, bem como a largura de material removido. Alguns defeitos que surgiram durante os cortes são também apresentados e discutidos.

Foi concluído que o aumento da velocidade de corte provoca um aumento da rugosidade e do ângulo de afunilamento das paredes, e uma diminuição na espessura de material removido. A orientação de corte não afectou a espessura de corte, mas foram registadas influências deste parâmetro aquando da medição do ângulo de afunilamento das paredes de corte e da rugosidade. Alguns defeitos como micro fracturas na zona de saída do jacto e fibras parcialmente cortadas foram observados para certas condições de corte.

Palavras-chave: Fibra de carbono, Rugosidade superficial, Defeitos, Corte por jacto de água, Velocidade de corte, Orientação de corte.

Abstract

Although composite materials have several advantages when compared to others, especially when their applications require high mechanical resistance/weight ratios, the prices limit their use to some applications.

Carbon fiber reinforced polymer, commonly known as carbon fiber, is a hard to cut material using conventional methods such as milling and sawing. Whereby the waterjet technology has gained importance in this field, since it does not suffer from high tool wear, do not create heat affected zones and is dustless. However, when cutting with waterjet some typical characteristics appear on the kerf walls, which, depending on the dimension, can be considered as defects.

Accordingly this work is intended to study the influence of the traverse rate and the cutting direction on the kerf taper wall, kerf width and surface roughness. To fulfill these purposes several cuts using different traverse rates and cutting directions were made, and the mentioned characteristics were measured. Some defects appeared during the cutting process and are also mentioned and discussed.

It was concluded that the cutting speed has a positive correlation with both the kerf taper angle and roughness, while a contrary trend was seen in the kerf width. The cutting direction did not affect the kerf width, while some influences were found on the measured values of both the kerf taper angle and roughness. Some defects such as fiber cracking at the exit point of the jet and fiber pullout were registered during the experimental procedure for certain operation conditions.

Keywords Carbon fiber composite, Roughness, Traverse rate, Abrasive Water Jet Cutting, Cut direction, Defects.

Index

Figure Index.....	vii
Table Index.....	ix
Nomenclature and Acronyms	x
NOMENCLATURE	x
ACRONYMS	x
1. Introduction	1
2. The abrasive water jet machining process	4
2.1. Introduction.....	4
2.2. Application fields.....	5
2.3. Operation parameters	5
2.4. Cutting	7
2.4.1. Jet lag.....	7
2.4.2. Kerf width variation.....	7
2.4.3. Surface waviness	9
2.4.4. Cutting Layered Composites	12
2.4.5. General trends of the cut characteristics with the operation parameters	15
2.5. Drilling small holes / Piercing	15
2.5.1. Delamination	16
3. Experimental setup and procedure.....	17
3.1. Introduction.....	17
3.2. Cutting equipment.....	17
3.2.1. Waterjet Machine	17
3.2.2. Software.....	18
3.2.3. Fixture.....	18
3.3. Abrasives	18
3.4. Workpiece Material	20
3.5. Piercing test.....	21
3.6. Experimental Design.....	22
3.6.1. Cutting Parameters	22
3.6.2. Cut design	24
3.7. Measurements	26
3.7.1. Roughness.....	26
3.7.2. Kerf taper angle	26
3.7.3. Kerf width.....	28
3.7.4. Waviness.....	29
3.7.5. Chain of procedures.....	29
4. Results and Discussion	30
4.1. Surface quality	30
4.1.1. Waviness.....	30

4.1.2. Surface roughness.....	31
4.2. Kerf taper angle	35
4.3. Kerf width	37
4.4. Piercing testing	40
4.5. Defects created during the experimental cuts	42
4.5.1. Surface Chipping	42
4.5.2. Fiber partially cut	44
4.5.3. Cracking – Exit point.....	45
4.5.4. Fiber pullout	45
4.6. Problems during the AWJC	46
4.6.1. Workpiece fall into the water tank	46
4.6.2. Frosting and surface scratches	47
4.6.3. Geometrical defects	49
5. Conclusions	50
5.1. Future work guidelines	52
6. References.....	53
Appendix A – Waterjet Glossary	55
Appendix B – Chain of Procedures	56
Appendix C – Piercing Measurements	57

FIGURE INDEX

Figure 1. Kerf taper geometries obtained by cutting using AWJM.....	7
Figure 2. Relative strength zones of the waterjet. The effective width/diameter of the jet depends of the workpiece material, since it represents the zone of the jet where there is enough energy to erode the material. Image taken from the work developed by Shanmugam and Masood (2009).....	10
Figure 3. Elements of the surface topography of a given surface. The surface profile is the combination of the waviness plus the roughness.....	11
Figure 4. Mechanism of delamination in order of occurrence: a – fracture initiation; b – water wedging; c – abrasive embedment and further cracking. Image taken from the work developed by Shanmugam <i>et al.</i> (2008).	14
Figure 5. Possible hole geometries obtained with AWJ. Figure taken from the work developed by Hashish (2011).....	16
Figure 6. Fixture system: a – detail of the used clamp system to avoid sideways movement; b – example of the placement of weights to avoid vertical movements.....	18
Figure 7. Detail of the HPX [®] abrasives series. Image retrieved from the catalogue of the manufacturer available at www.barton.com	19
Figure 8. Cutting direction used on the present work. The 0° direction corresponds to cutting along the direction of the top layer fibers.	22
Figure 9. Type A cuts. These cuts were made in order to measure the surface roughness and the kerf taper angle variation with cutting direction. The A1 cuts focus in 0°, 45°, 90° and 135°, while the A2 cuts focus in the 22.5°, 67.5°, 112.5° and 157.5° cutting directions. SP and EP stand for, respectively, Start Point and End Point of the tool path.	24
Figure 10. Type B cuts. These cuts were made in order to measure the top kerf width variation with the cutting direction. The presence and magnitude of minor defects such as surface chipping were also analyzed. The B1 cuts focus in 0°, 45°, 90° and 135°, while the B2 cuts focus in the 22.5°, 67.5°, 112.5° and 157.5° cutting directions.....	25
Figure 11. Schematic view of the sampling length (path) for the 3 kerf wall depths.....	26
Figure 12. Fixation system used to measure the kerf angle of the cut: a – detail of the fixation holes drilled on the samples; b – sample fixed to the aluminum support; c – fixation system bolted to the CMM.	27
Figure 13. Zone suitable for kerf taper angle measurement, represented by the black and white stripped pattern. The orange line represents the path taken by the CMM and the black dots the points that led to this path.	28
Figure 14. Transition between the smooth cutting zone (cutting wear zone) and the rough cutting zone which presents waviness: a – Rst 37.2 (DIN 17100) steel 6 mm thick cut at a traverse speed of 500 mm/min (retrieved from the work made by Dias, 2011); b – carbon fiber cut at 2000 mm/min with a cutting orientation of 45°; c - carbon fiber cut at 1500 mm/min with a cutting orientation of 45°.	31

Figure 15. Roughness variation with the cutting direction and cut depth, at the four different traverse speeds: a – 2000 mm/min; b – 1500 mm/min; c – 1000 mm/min; d – 500 mm/min.	32
Figure 16. Roughness variation with the cutting direction and traverse speed, for the three different cut depths: a – 1 mm; b – 2.2 mm; c – 3.5 mm.	34
Figure 17. Variation of the average values of R_a with the traverse speed [mm/min] and the cut depth.	35
Figure 18. Kerf taper angle variation with the cutting orientation and traverse speed. Traverse speed in mm/min.	36
Figure 19. Kerf width variation with the traverse speed: black line – top kerf width; green line – bottom kerf width.	39
Figure 20. Slowing down effect on the top kerf width and maximum kerf width measurement at a rated traverse speed: a – 500 mm/min; b – 2000 mm/min. Pictures taken using an optical microscope with a digital camera connected to a computer with a magnification of 10X.	40
Figure 21. Damage created by the tested piercing methods at the surface of the plate: 1 – Delaminate carbon fibers; 2 – Pullout of the polyamide/glass fibers; 3 – Carbon fiber cracking; 4 – uncut carbon fiber. The white arrows represent the direction of the piercing and are the same for all the dynamic piercing photos. Scale: 1 mm.	42
Figure 22. Surface chipping on the entry jet zone made by AWJ cutting. Cutting direction of 45° and traverse speed of: Left photo – 2000 mm/min; right photo – 1000 mm/min. The red arrow represents the cut direction and the dashed orange line the top layer fibers orientation. Photos taken with an optical microscope with a camera connected to a computer and a magnification of 10X. Scale: 500 μm . .	43
Figure 23. Angles between the cut direction and the fibers. With this cutting conditions surface chipping would occur mainly on the right side since $\theta < \beta$	44
Figure 24. Flaws that occurred at the exit point: partially cut polyamide fibers and cracking. The left cut was made with a traverse speed of 500 mm/min and the right one at 1000 mm/min. Both cuts performed with $\theta = 45^\circ$	45
Figure 25. Flaws created near the entry jet point. Label: 1 – Polyamide fiber; 2 – Glass fiber.	46
Figure 26. Defects created at the bottom of the plate during the AWJM at 500 mm/min: 1 – gap created by long exposure to the jet splash back; 2 – Frosting due to jet splash back on the support slats; 3 – scratches created at the support slats/plate interface.	48
Figure 27. Schematic representation of the problems felt during the AWJC due to bad fixture.	49
Figure 28. Chain of procedures regarding the experimental cuts and measurements.	56
Figure 29. Schematic view of the elliptical affected area, caused by piercing.	57

TABLE INDEX

Table 1. General trend of the cut characteristics with the increase of the most important cut parameters. Arrows pointing up, down and sideways means, respectively, increase, decrease and no variation for a given cut characteristic. Two opposite arrows mean that there are different conclusions about that parameter. The question mark means that no information was found.....	15
Table 2. Typical particle size distribution of the HPX [®] 80 abrasives. Values provided by the manufacturer of the abrasive, BARTON.....	19
Table 3. Major properties of the test material.....	20
Table 4. Design of experimental parameters for the cutting process.....	24
Table 5. Top kerf width values obtained from the microscope measurements. Kerf width values in microns.....	38
Table 6. Bottom kerf width values calculated from the top kerf width measurements and kerf taper angle measurements. Kerf width values in microns.	38
Table 7. Conditions of the prediction rule for the surface chipping side. The chipping side refers to the right or left side when facing the cutting direction.	44
Table 8. Affected areas created by the tested piercing methods. L.P. stands for “Low Pressure”. The piercing methods are sorted by top affected area size, low to high.	57
Table 9. Measured kerf angles in degrees.....	58

NOMENCLATURE AND ACRONYMS

NOMENCLATURE

A_{AP} – Area affected by piercing [mm^2]

K_T – Kerf taper angle [degree]

$K_{W,B}$ – Kerf width at the bottom [μm]

$K_{W,T}$ – Kerf width at the top [μm]

$u_{C,T}$ – Critical traverse speed that allows taper free cuts [mm/min]

h – Plate thickness [mm]

R_a – Average roughness [μm]

a – One-half of the ellipse's major axis [mm]

b – One-half of the ellipse's minor axis [mm]

β – Cutting direction angle, measured at the left side [degree]

θ – Cutting direction angle, measured at the right side [degree]

φ – Striking angle of the water jet [degree]

ACRONYMS

ACAB – Applied Composites AB

AWJ – Abrasive Water Jet

AWJC – Abrasive Water Jet Cutting

AWJM – Abrasive Water Jet Machining

CMM – Coordinate Measuring Machine

CRFP – Carbon Fiber Reinforced Polymer

CT-Scan – Computed Tomography Scan

DEM – Departamento de Engenharia Mecânica

FCTUC – Faculdade de Ciências e Tecnologia da Universidade de Coimbra

HAZ – Heat Affected Zone

LiU – Linköping University

WEDM – Wire Electrical Discharge Machining

1. INTRODUCTION

Since the beginning of Mankind we seek means to move goods and people faster, more reliably and lately at the least cost. We invented mechanical principles like the wheel which allowed the appearance of animal powered vehicles. In the beginning both the wheels and the vehicles were made basically of wood. However, over the years, with the increasing demand for faster and more reliable vehicles other inventions took place like the internal combustion engine. With these inventions, new materials are now used, and obviously the woodworking tools like axes, chisels and saws are no longer suitable to give shape to new materials like steel and iron.

In the last few years, with the generalization of personal transportation and the increased use of air transportation to move people and goods, the use of new materials, such as carbon fiber reinforced polymer composites, is required by transport industries (aviation, automotive and maritime industries).

Carbon fiber reinforced polymer composite (CFRP), commonly referred as carbon fiber, is known for having high resistance to water corrosion, being capable of displaying different mechanical properties according to fiber orientation, and having a high tensile strength associated to a low density, giving them a high strength-to-weight ratio. However, due to the difficulty to automate the current manufacturing techniques and its post processing needs, this kind of materials are typically expensive, being its use reserved mainly for highly demanding applications where the extra cost of the material is worth due to the savings resulting from the weight reduction. This is a common situation in the transport industries.

Cutting carbon fiber with traditional tools like saws creates several problems such as the production of large amounts of dust, high tool wear and Heat Affected Zones (HAZ). Although these problems can be partially solved with the use of coolants, the physical and chemical reactions with the material are always uncertain. Other problems arise like fiber pullout, delamination, low cut rates and cracking. Therefore, like it happened before with the stone to metal evolution, new tools are needed.

This is where the abrasive waterjet technology gains importance by being a dustless and heatless process, able, at the same time, of cutting at high rates. The consumables are mainly tap water and garnet, which are largely available everywhere at reasonable prices. Also the material removal process is universal for all the materials, which leads to great flexibility of the process.

However, the Abrasive Water Jet (AWJ) technology has some drawbacks that may avoid its use when tight tolerances are required. Typically it creates tilted kerf walls (*kerf taper angle*), and, in certain conditions, waviness appears on the kerf walls. The amount of removed material (*kerf width*) may also be a problem since it is highly dependent on the cutting speed. Thus, it may become necessary to change the cutting speed during the cut operation in order to avoid dimensional variations at the exit point of the jet due to the jet deflection. When cutting inhomogeneous materials such as carbon fiber, different cutting direction lead to different cutting conditions which can have influence on the mentioned characteristics.

The purpose of this work is to ascertain the influence of both the cutting direction and cutting speed on the kerf taper angle, kerf width and surface roughness at different cut depths, when cutting a carbon fiber plate. In order to fulfill this objective several cuts have been performed with different cut directions and speeds, and measures were later taken to ascertain the magnitude of the mentioned characteristics.

Some problems due to the waterjet machine characteristics arose, such as workpiece fall into the water tank and frosting and surface scratches on the lower surface due to the jet back on the support slats. The found solutions, as well as other alternatives, are presented and discussed later in this work.

The experimental part of the work was developed at Linköping University (LiU), in Sweden, at the Production Systems division of the Department of Management and Engineering.

This work is divided in 4 main Chapters:

In Chapter 2 a brief resume of the abrasive water jet technology potential and more common issues is made, as well as the general trends of the studied characteristics with the most usually changed operation parameters.

Chapter 3 is dedicated to the working methodologies and describes the workpiece material, the used waterjet machine and the experimental procedure used in the present study, as well as the measurement procedures and used measuring devices.

The results of this study and its discussion are made in Chapter 4, while a resume of the conclusions can be seen in Chapter 5. In this last chapter a few guidelines that may be followed for future works in the field are also proposed.

2. THE ABRASIVE WATER JET MACHINING PROCESS

2.1. Introduction

Cutting with AWJ technology is a non-traditional method and is one of the fastest growing machining processes in the last decades. AWJ cutting competes in its class with other cutting processes such as plasma, oxy-fuel, Wire Electrical Discharge Machining (WEDM) and laser cutting. Its main advantages are:

- The ability of cutting different materials with minor or none response to its properties like electrical conductivity and reflectivity, which respectively affect the WEDM and laser cutting (Zheng *et al.*, 1996);
- Environmental friendliness, since the most used consumables are basically tap water and sand;
- Being capable of cutting thicknesses up to 400 mm (Orbanic and Junkar, 2007);
- Since it is a non-thermal process there is no HAZ;
- It is a non-solid contact method so there is no tool wear. Nevertheless the nozzle parts may require maintenance or replacement each few hundreds of hours;
- Virtually able to cut any material, since the process of material removal is considered to be universal and therefore independent of the material. Very brittle materials may be a problem since they break upon the jet impact on the workpiece;
- Causes low stresses on the material when compared with other methods.

However, the process has some characteristics that cause inaccuracies, e.g. the variation of the kerf width with the cut depth and the striation formation on the surface of the cut. These issues are explained later on this work, as well as the operation parameters that may have direct influence on them. Also, since the process typically depends directly on the use of water, some corrosion may occur, especially on metallic materials.

2.2. Application fields

The water jet process has proved to be worth in several applications from the medical and the food industries to aerospace and automotive industries. The most current applications within these areas are the cut of carton, car carpets, aircraft fuselage, and cardboard and even stripping and cutting of fish and other food.

Upon the use of solid particles in the jet stream, the so-called abrasives, the range of applications became even wider allowing the machining of thicker and harder to machine materials with higher removal rates.

Nowadays the abrasive water jet technology is used in several processes (Hashish, 2011 and Folkes, 2009), some already well diffused in the industry and others that are still emerging:

- *Cutting* – the jet is used to cut through the material;
- *Drilling* – the jet pierces the material creating a hole. The shape of this hole is discussed later on this work;
- *Milling* – although with some limitations, the jet is used to remove material to a specific depth;
- *Turning (lathe)* – the jet is used to create a surface of revolution;
- *Jet assist* – the jet is used to assist other material removal processes: cooling, lubrication and chip removal;
- *Changing surfaces conditions* – the jet is used to remove paint, dust, rust and to change the surface texture like polishing and texturing. Coatings removal is also possible.

2.3. Operation parameters

There are some parameters that have a direct influence in the waterjet cutting performance known as operation parameters. The most common parameters regarding the waterjet cutting can be divided into groups (ÖJmertz, 2006) which are:

- **Cutting Parameters**
 - *Traverse rate* – relative speed between the workpiece and the nozzle. Also known as feed rate, cutting speed and traverse speed;

- *Stand-off distance* – distance between the nozzle and the workpiece;
- *Striking angle* – angle between the workpiece surface and the waterjet nozzle;
- **Hydraulic Parameters**
 - *Water pressure*
 - *Waterjet diameter*
- **Mixture Parameters (Abrasive Waterjet only)**
 - *Abrasive flow rate*
 - *Abrasive particles size*
 - *Abrasive particles geometry*

The cutting parameters are the easier to vary, because normally it only requires a few changes in the machine software, especially in newer machines thanks to the growing automation of the nozzle movements.

The water pressure can be changed easily as well, but it may not be worthwhile due to design limitations of the pressure system, loss of efficiency and increased maintenance since the machine is not operating at the nominal pressure.

In order to change the mixture parameters it is required to have different kinds of abrasives, clean the abrasive hopper and the feed lines upon the change of the abrasive, and if the new abrasive particles are too big clogging may occur, forcing the change of the focusing tube by a larger one, which increases the jet diameter. Typically, when using coarser grades of abrasives the cutting speed is increased but a rougher cut surface is obtained. The opposite takes place when a finer mesh size is used, which means that the cut surface is smoother although cutting at lower speeds (Folkes, 2009).

Upon the cutting of anisotropic materials, such as laminate composites a new machining parameter arises: the cutting direction. So, if an equal quality is required along all directions, some operation parameters may need to be tuned depending on the cutting orientation.

2.4. Cutting

Some phenomena occur when cutting with AWJ technology, which leads to the appearance of some typical features on the workpiece. These features can be considered as defects depending on their magnitude or end use of the part. Therefore, it is important to know which operation parameters affect these phenomena, in order to control their magnitude or occurrence.

2.4.1. Jet lag

When cutting through a material, the jet is deflected opposite to the cutting direction. This means that the jet exit point lags behind in relation to the jet entry point. The horizontal distance between these two points is typically called lag, drag or trailback. The drag magnitude is highly dependent on the traverse speed: greater traverse speed lead to greater lag distance.

So if cutting at high speed it might be required to slow down the jet when reaching the end of a tool path or in small radius curves, in order to avoid geometrical flaws at the bottom of the workpiece due to the jet deflection.

2.4.2. Kerf width variation

The kerf with represents the distance between the two walls created upon the cutting. It is one of the characteristic of the process because the kerf width varies along the cut depth. This variation is often called the kerf taper angle or simply taper. The kerf taper angle can be positive, neutral or negative, depending if the kerf width at the bottom is lower, equal or higher than the top kerf width, as seen in Figure 1.

When cutting thick materials the kerf walls can get rounder, showing the shape of a barrel. The barrel shape can be combined with negative, zero or positive kerf taper angle.

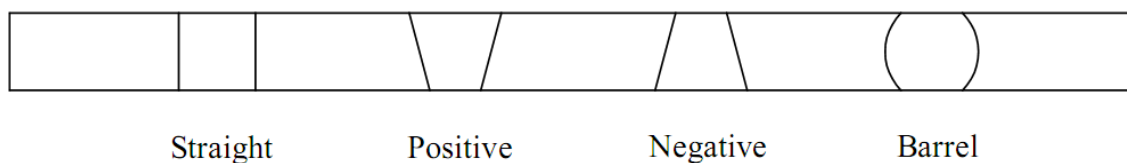


Figure 1. Kerf taper geometries obtained by cutting using AWJM.

The kerf taper angle may change upon the variation of some operation parameters, which means that the relationship between the top and bottom kerf width is not constant. For example, when increasing the water pressure, despite both the top and bottom kerf width increase approximately linearly, the kerf taper angle also increases as shown in the study developed by Wang (1999). So the kerf width and the kerf taper angle are often analyzed as two different problems.

2.4.2.1. Kerf width

The kerf width can be defined in every available controller and it is normally represented as the tool offset. This parameter can create systematic dimensional errors if defined wrongly, so it is rather important to know its magnitude and range for different operation parameters. It is also important to bear in mind that the current controllers may consider the tool offset to be either the kerf width value or half of it.

Although the top and the bottom kerf width can present different rates of variation with a given operational parameter, the signal of that variation is typically the same, which means that when one increases the other increases as well, even if at different rates. So from the studies made in the field, it is possible to say that the top kerf width:

- Decreases with the increase of *traverse speed*, as show in the study made in polymer matrix composites by Wang (1999). This happens because a higher traverse speed allows fewer abrasives to strike on the material which creates a narrower slot;
- Increases with the increase of the *stand-off distance* (Wang, 1999). Although the bottom kerf width seems to increase at a slower rate than the top one. This can be explained by the decrease of the effective diameter with the jet length, as shown in Figure 2;
- Shows little to no variation in relation to the *abrasive flow rate*, as show in the study developed by Shanmugam and Masood (2009) in layered composites (carbon/epoxy and glass/epoxy).

2.4.2.2. Kerf taper angle

The kerf taper angle is a major problem when cutting with AWJ technology, and the main solutions are the decrease of traverse speed until a critical value that creates taper free cuts, or using compensation techniques. The most used compensation is to tilt

the nozzle. This technique can only eliminate the taper on one kerf wall, while the kerf taper angle of the opposite wall may even increase.

Although cutting at the critical speed $u_{c,T}$ can produce taper free cuts, it reduces the productivity to unbearable levels. So, since the tilting technique allows the cutting at normal traverse speeds creating taper free cuts at the same time, it is a better solution when only one of the kerf walls is required to have zero taper.

According to the study developed in alumina ceramics by Shanmugam *et al.* (2008.b), the kerf taper angle varies almost linearly with the tilting of the nozzle. But in order to compensate the taper angle, it is necessary to know the parameters that affect the kerf taper angle. The taper of a cut:

- Do not change with the *abrasive flow rate* as shown by Shanmugam and Masood (2009);
- Increases with the increase of *the stand-off distance*. As this distance increases, the jet diameter increases as well until a certain point, from which it decreases quickly. So at the bottom of the kerf the jet may be already decreasing which makes the top kerf width smaller than the bottom kerf width. This model is supported by Shanmugam and Masood (2009) and Wang (1999);
- Increases with the *traverse speed* if it is higher than the value of $u_{c,T}$ or decreases if cutting at slower speeds because the kerf taper angle is negative. This trend is supported by Shanmugam and Masood (2009) in their work, and it was verified by the present work. However there is some controversy in this field because some studies, like the one made by Wang (1999), say that the kerf taper has little to no dependency on the traverse speed;
- Does not have a conclusive relationship with the *water pressure*. According to the measurements performed by Shanmugam and Masood (2009) the taper reduces with the increase of the water pressure, while Wang (1999) concluded the opposite.

2.4.3. Surface waviness

Surface waviness formation is a hard to explain process since it is a dynamic tridimensional phenomenon and occurs due to the interaction between the workpiece and

the waterjet, which travels at speeds up to 800 m/s. This is one of the main disadvantages of cutting with AWJ technology. Several studies have been made to explain the process, but none of them have provided a full description of it, or even consensual. Nevertheless an overview of the proposed striation formation mechanisms is made below.

According to Hashish (2011), the surface waviness phenomenon occurs because the jet/material interface is not steady. When the jet is eroding a piece of material from the top to the bottom, the nozzle keeps moving and the effective diameter of the jet reduces with the cut depth increase as show in Figure 2 . Since this turns out to be a cyclic process, waviness appears on the kerf walls.

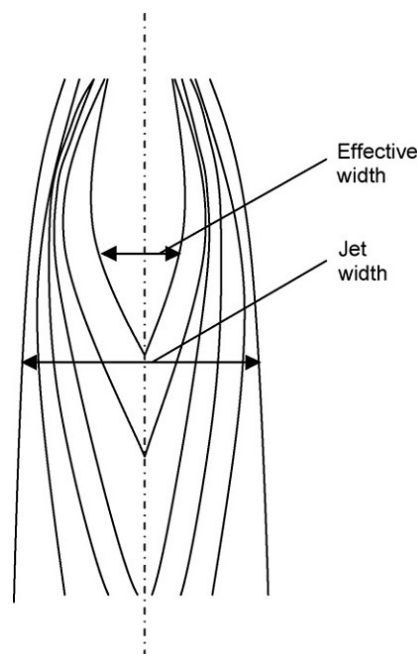


Figure 2. Relative strength zones of the waterjet. The effective width/diameter of the jet depends of the workpiece material, since it represents the zone of the jet where there is enough energy to erode the material. Image taken from the work developed by Shanmugam and Masood (2009).

Other studies relate the striation phenomenon with the vibrations during the cutting process and uneven distribution of the kinetic energy of abrasive grains inside the AWJ, as referred by Orbanic and Junkar (2008) on their study. Nevertheless, all these authors agree that with the current state of AWJ technology it is not possible to eliminate completely the striation formation. However, when cutting at slow speeds the increased jet overlapping can eliminate some of the striation from the cut surface.

2.4.3.1. Surface quality

The criteria to evaluate AWJ machined surfaces has been the magnitude of the two main parameters that characterize the topography of a given surface (Figure 3.a) which are: roughness (Figure 3.c), consisting in closely spaced irregularities created by the cutting tool marks, abrasives or grinding wheels, and waviness (Figure 3.b), that are more widely spaced irregularities normally associated with vibrations and jet destabilization. Typically, the smaller these parameters are, greater the surface quality.

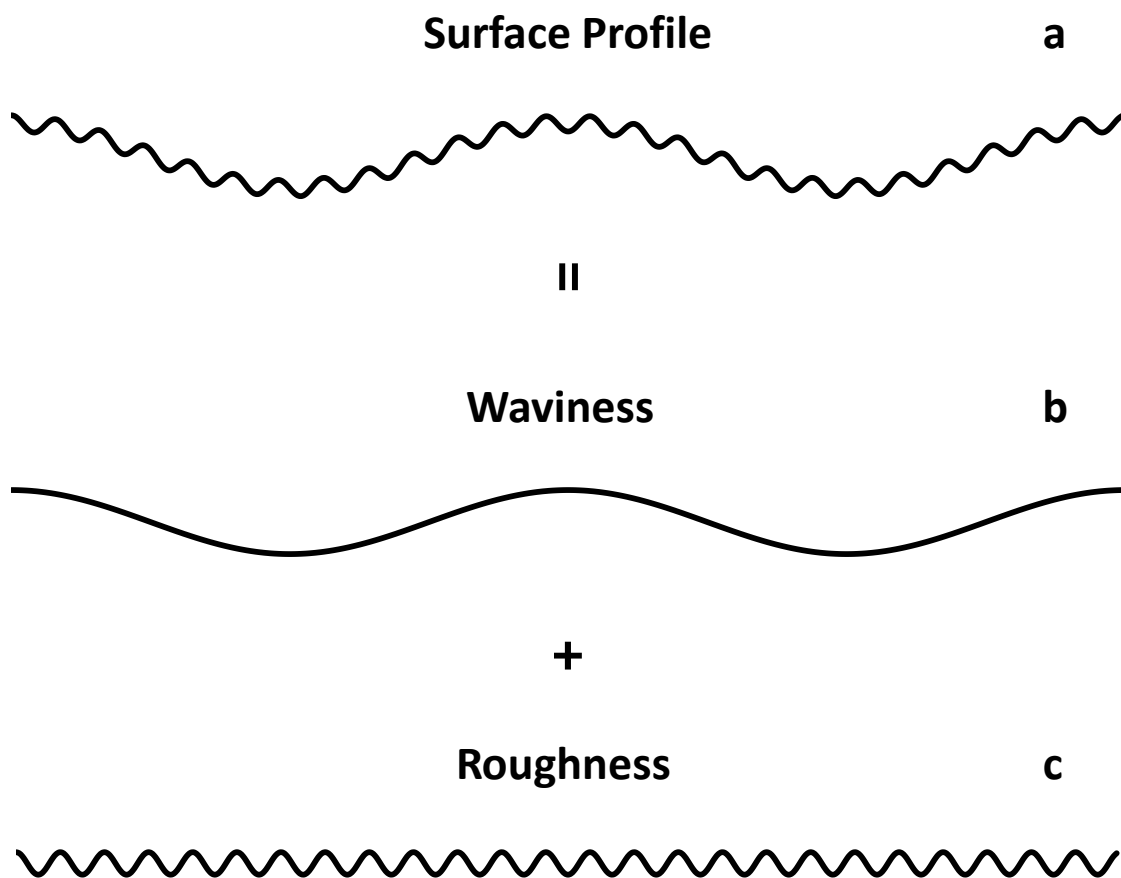


Figure 3. Elements of the surface topography of a given surface. The surface profile is the combination of the waviness plus the roughness.

The kerf wall can be divided in two main areas (Wang, 1999), taking into account its topography: the area right next to the entry point of the jet, called the cutting

wear zone (micro defects), where the roughness is the most important factor, and the area called deformation wear zone (macro defects), where the waviness dominates.

If the cut is made too fast the waviness starts to appear at the bottom of the kerf wall and at some point the surface finish gets too rough for most the applications, and eventually the jet will not even cut through all the material.

The cutting wear zone length is directly related to the energy available on the jet, so it is possible to avoid the most of this waviness if certain operation conditions are used in order to increase the jet energy, like increasing the jet pressure or decreasing the traverse speed (Wang, 1999)

Yet, regardless of the chosen operation conditions, the surface quality has a tendency to deteriorate as the depth of the cut increase (Akkurt *et al.*, 2004). With the increase of the cut depth, the jet loses energy due to the energy spent in the cut of the upper material, abrasive particles interactions and friction between the jet and the surrounding air (water if the cut is made underwater), which results in greater roughness on the bottom surfaces.

Taking into account the studies made in the AWJM field, it is possible to say that the surface roughness of the kerf walls:

- Is lower with decreasing *traverse speed* (Akkurt *et al.*, 2004), since with a slower speed more jet overlapping is likely to occur;
- Is not dependent on the *stand-off* distance and abrasive mass flow rate if reasonable values are used (Wang, 1999; Azmir and Ahsan, 2008);
- Is lower when using harder abrasive materials (Azmir and Ahsan, 2008).

2.4.4. Cutting Layered Composites

Layered composites, such as carbon fiber, are inhomogeneous materials due to its matrix properties, fiber orientation and relative volume fraction of matrix. They may also possess low inter-laminar bonding and very high tensile strength. When cutting or drilling layered composites some problems may occur such as delamination, edge chipping and crack formation. Of these, delamination has been identified as the most harmful to the material (Ramulu *et al.*, 2009).

2.4.4.1. Delamination

According to Shanmugam *et al.* (2008.a), there are two major actions during the waterjet cutting: one is the erosion process that removes material within the active region of the jet, and the second consists on applied stresses on the generated kerf walls. This applied stresses are a result of the imprisonment of the jet between the kerf walls.

So, as shown in Figure 4.a-c, the mechanism of delamination has three main stages:

1. *Fracture initiation* – due to the low material removal rate there is enough time for the cracks to initiate by the shock wave impact of the waterjet;
2. *Water-wedging* – after the cracks are generated, the applied stresses by the jet on the generated kerf walls allows the water flow to enter the crack tips and develop a water-wedge action, causing the propagation of the cracks;
3. *Abrasive embedment and further cracking* – with the introduction of abrasive particles further wedging occur and some particles are trapped inside the cracks. When the delay time between the introduction of the abrasive particles and the start of the cutting is reduced or nonexistent the two last stages occur at the same time.

However, when cutting with AWJ the jet has more power, and therefore is more likely to cut through the part. In these conditions the available area for the jet to escape is greater, which reduces the applied stresses on the generated kerf walls. Therefore the number of cracks and their propagation length is reduced as well, as shown in Shanmugam *et al.* (2008).

So it is possible to say that the delamination phenomenon is highly dependent on the capacity of the jet to penetrate on the material. In fact, it seems that delamination only occur when the jet is unable to cut through the workpiece. This possibility is supported by the work made by Wang (2002), where a model to predict the depth of penetration when cutting polymer matrix composites was created. This model says that the depth penetration increases with the water pressure and the abrasive feed rate, while the traverse speed has a reverse effect.

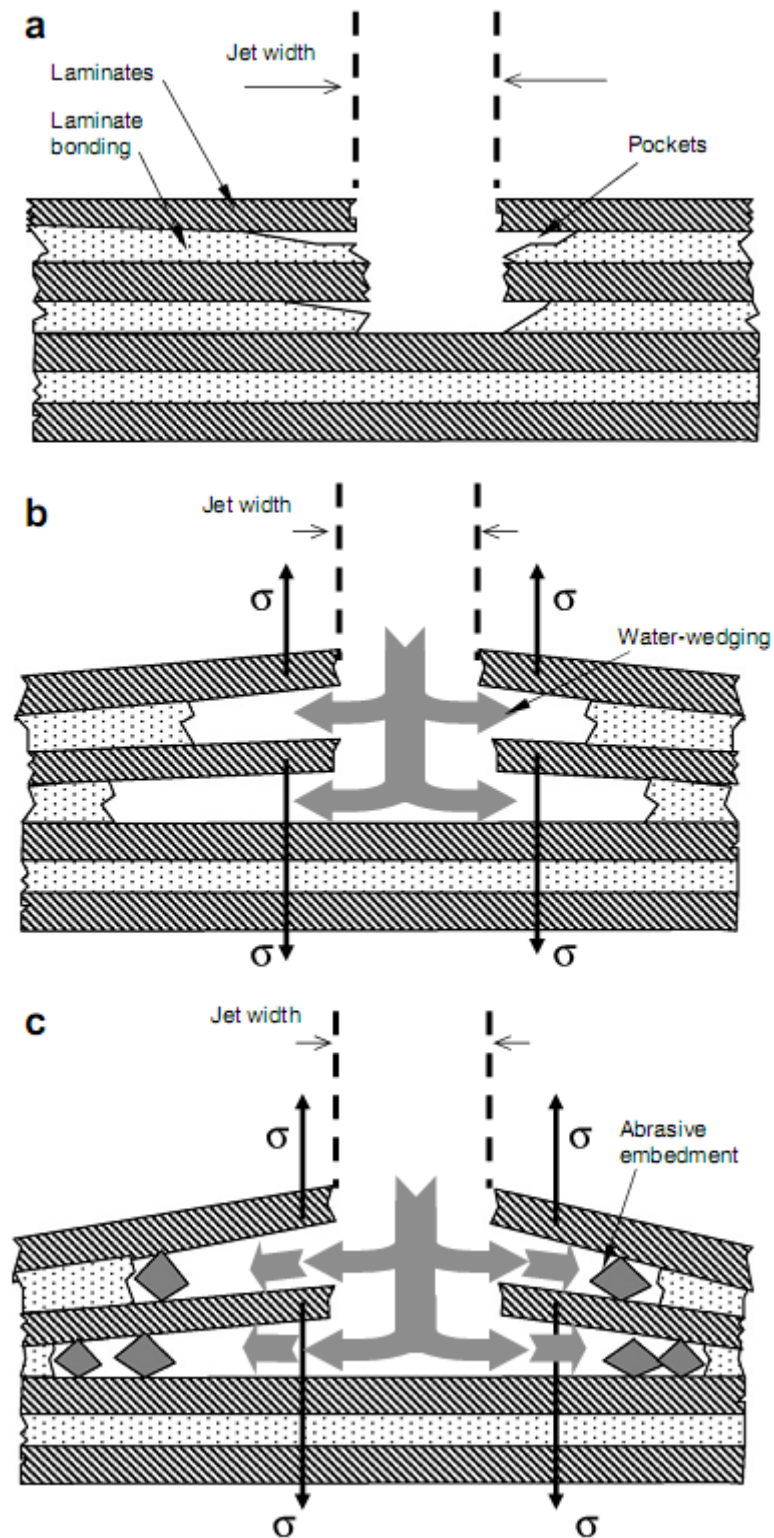


Figure 4. Mechanism of delamination in order of occurrence: a – fracture initiation; b – water wedging; c – abrasive embedment and further cracking. Image taken from the work developed by Shanmuganm *et al.* (2008).

2.4.5. General trends of the cut characteristics with the operation parameters

A resume of the general relationship between the cut characteristics and the most important cut parameters is shown in Table 1. As shown there are few tests performed on this technical field to analyze the influence of the cut orientation on the characteristics of the cut.

Table 1. General trend of the cut characteristics with the increase of the most important cut parameters. Arrows pointing up, down and sideways means, respectively, increase, decrease and no variation for a given cut characteristic. Two opposite arrows mean that there are different conclusions about that parameter. The question mark means that no information was found.

<i>Operation Parameters</i>	<i>Roughness</i>	<i>Delamination</i>	<i>Kerf taper angle</i>	<i>Kerf width</i>	<i>Penetration depth</i>
Water Pressure	↓	↓	↓ ↑	↑	↑
Stand-off	↑	↑	↑	↑	↓
Traverse Speed	↑	↑	↑ →	↓	↓
Abrasive Flow Rate	↓	↑	→	?	↑
Cutting Orientation	→	?	?	?	?

It is important to bear in mind that almost all the studies done in the AWJM field have empirical or semi-empirical approaches. So, if the range of operation parameters and/or materials is very different from the used on those studies, the mentioned trends may be different.

2.5. Drilling small holes / Piercing

As with cutting, when drilling with AWJ technology some problems may arise. The kerf width variation with the depth of the cut is still an issue, which creates some different configurations of the kerf walls, as shown in Figure 5. As the jet penetrates into

the material, the return flow is also exiting the material since it is the only escape path. This may cause secondary erosion on the kerf wall, which increases the final diameter of the hole, and reduces the jet speed at the same time. The combined effect of these two phenomena directly affects the final shape of the hole.

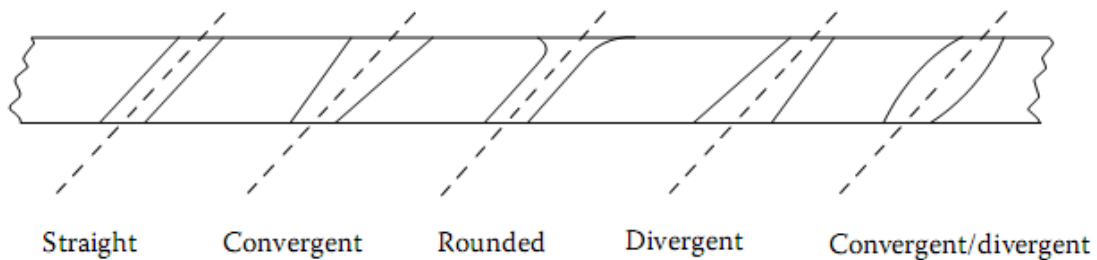


Figure 5. Possible hole geometries obtained with AWJ. Figure taken from the work developed by Hashish (2011).

Although drilling with AWJ has several advantages like no wear of the tools (it is a toolless process), no HAZ and the ability to create holes with different shapes if tilting nozzle abilities are available, some problems may occur when piercing layered composites or brittle materials such as glass. These problems include delamination and fracture of the material, and are well known and already studied in several works like the ones made by Liu and Schubert (2009) and Ramulu *et al.* (2009).

2.5.1. Delamination

According to Shanmuganm and Masood (2009), delamination occurs when high stresses capable of separating the layers of material are applied to the kerf walls. While piercing, the jet is imprisoned in the created hole, so the referred stresses on the kerf walls are high. It is believed that the applied stresses are even higher if compared to the ones created while cutting without pierce, since the water only has one direction to exit (upwards), in contrast to the two directions when cutting (upwards and sideways within the generated kerf walls).

3. EXPERIMENTAL SETUP AND PROCEDURE

3.1. Introduction

In this chapter it is possible to find a description of the equipments and the methodology followed in the creation of the specimens and measurements of the surface roughness, kerf taper angle and kerf width. The cut material characteristics are also presented in this section.

3.2. Cutting equipment

The waterjet equipments produced nowadays have a modular design, which means the buyer can customize his machine choosing from a large list of nozzles, movement controllers, cutting tables, pressure pumps, control software and other accessories like nozzle tilting mechanisms and multiple nozzles in order to increase productivity.

3.2.1. Waterjet Machine

The experimental cuts were made on an OMAX[®] JetMachining[®] model 5555 equipped with a direct drive EnduroMax[®] pump, with a nominal pressure of approximately 380 MPa (55 kpsi). All the axes were motorized and capable of moving the nozzle at maximum speed of 4572 mm/min with ballbar circularity (over 300mm) of 0.08 mm.

The nozzle was equipped with a tilting mechanism (Tilt-a-Jet[®] from OMAX[®]) capable of tilting up to nine degrees in any direction, which allows the use of compensation to eliminate the taper or create angled kerf walls. Although the software predicts the generated taper angle, if taper free parts with tight tolerances are required it might be necessary to run some trials to tune the tilting angle and the tool offset. For the present work, this tilting ability was not used.

The machine was brand new, and at the time of the last experimental cut the machining time counter showed less than 5 working hours. So the typical problems arising from nozzle parts wear like lost of jet focus and circularity are not expected to occur.

3.2.2. Software

The software used to design the cuts was Intelli-MAX[®] Layout Premium V.17. The software used to control the machining process was the Intelli-MAX[®] Make Premium V.17. Both the programs were developed by the manufacturer of the waterjet machine and are normally supplied with the water jet equipment.

3.2.3. Fixture

The horizontal movements of the workpiece were constrained simply by putting weights on the top of it, while the constraint of the sideways motion required the use of a spacer to push the workpiece against the aluminum plates fixed at the corners of the catch tank, as shown in Figure 6. Since the reliability of this system depends on the interface between the material and the aluminum plates, it was important to guarantee that there were not any abrasives or other debris that could cause friction losses.

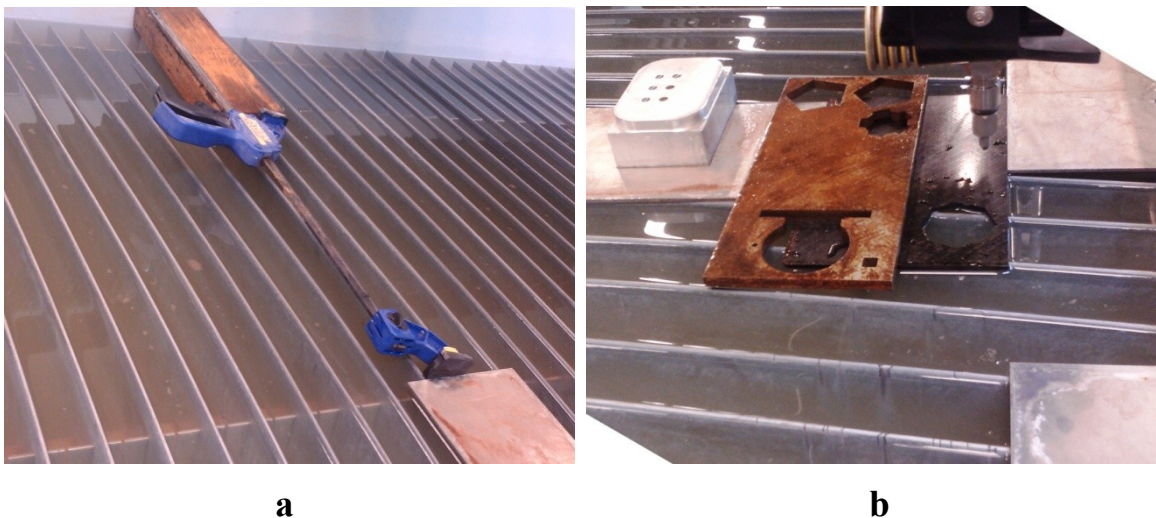


Figure 6. Fixture system: a – detail of the used clamp system to avoid sideways movement; b – example of the placement of weights to avoid vertical movements.

3.3. Abrasives

Industry type abrasive garnets with a mesh size of #80 were used for this study, as they are known to provide a good versatility for a wide variety of cuts and therefore are the most widely used in the industry.

The commercial name of the used garnet is HPX[®] 80 and was produced by BARTON. The average size of the particles, according to the manufacturer, was approximately 232 μm and the typical particle size distribution is show in Table 2.

Table 2. Typical particle size distribution of the HPX[®] 80 abrasives. Values provided by the manufacturer of the abrasive, BARTON.

		Screen size [US] / Opening [Micron]						
		45 / 355	50 / 300	60 / 250	70 / 212	80 / 180	100 / 150	115 / 125
% by weight		5	19	26	21	17	7	5

There are three major types of garnet abrasives when taking into account their origin: mined and collected from alluvial sources or sea. According to the study performed by Boud *et al* (2010), the mined garnets present sharper edges than the ones collected at the river, with the garnet obtained at the sea in the middle. Since the used abrasives were mined, it is considered that they have sharp edges, as shown in Figure 7.



Figure 7. Detail of the HPX[®] abrasives series. Image retrieved from the catalogue of the manufacturer available at www.barton.com.

3.4. Workpiece Material

Generally speaking, carbon fiber composites are known for having high tensile strength associated to a low density, giving them a high strength-to-weight ratio. However, due to the difficulty to automate the current manufacturing techniques, this kind of materials are typically expensive, being its use reserved mainly for applications where the extra cost of the material is worth due to the savings from the weight reduction. This is a common situation in the transport industries, which explains the growing use of carbon fiber in the aviation and the automotive industries.

A plate of laminate composite 4,4 mm thick and consisting of carbon fiber and epoxy resin was used. The material was made from a total of 16 layers, each layer being made from unidirectional carbon fibers, with glass fibers along the carbon fibers each 3 mm and polyamide fibers perpendicular to the carbon fibers each 7 mm.

The workpiece material was produced by ACAB (Applied Composites AB) using a technique called Resin Transfer Molding (RTM) which is considered to be suitable for mass production of parts with complex shapes and small tolerances. In order to increase productivity, the layers of carbon fiber were stacked and glued together with a mild binder (creating a preform) before going to the closed mold where a mixed resin and catalyst are injected.

The epoxy resin was produced by *Excel* and the commercial name is HexFlow[®] RTM6. This is a premixed epoxy resin capable of service temperatures from -60°C up to 180°C and designed to fulfill the requirements of the RTM process like low viscosity during the injection and long injection time window.

Table 3. Major properties of the test material.

Stacking Sequence [degrees]	[0/+45/-45/90]
Number of Layers	16
Volume fraction of the fiber	0.60
Laminate thickness [mm]	4.4
Average fiber diameter [μm]	8

3.5. Piercing test

It is known that piercing carbon fiber using AWJ technology should be avoided whenever possible, since defects such as delamination, cracking and fiber pullout often occur. Nevertheless there are a few different piercing methods that might improve piercing in carbon fiber or other brittle materials such as glass, some ceramics and other laminates. Among all the known piercing methods the most used are:

- *Stationary piercing* – the piercing is performed without moving the nozzle. This can be a problem, especially in thicker materials because as piercing occurs the water and abrasive mixture will go out backwards to the sides of the jet, which increases the diameter of the hole while slowing down the water jet. This makes the hole greater than the jet diameter. It is one of the slowest methods, but it is useful when the material to cut is expensive or there is no room to apply any other piercing method;
- *Dynamic piercing* – instead of performing the piercing without moving, the nozzle slowly cuts through the material until it reaches the desired cut path. The proper cutting parameters must be chosen when using this method in order to ensure that the piercing is already completed when it reaches the path;
- *Low pressure and water only dynamic piercing* – these ones were combined separately with the dynamic piercing method. Piercing at low pressures is normally used when cutting brittle materials, since the shockwave from the jet impact is smaller.

When testing the low pressure dynamic piercing the “brittle mode” available on the machining software was turned on. With this option turned on the pump pressure is raised slowly while piercing to avoid the sudden impact of the full pressure waterjet in the material. The low pressure value was 20 kpsi (137.9 MPa).

3.6. Experimental Design

3.6.1. Cutting Parameters

In order to fulfill the objectives of this study, the influence of two machining parameters was analyzed: cutting direction and traverse rate. All the other parameters were kept constant during the experiments.

3.6.1.1. Cutting direction

As referred previously, the cutting direction only turns out to be a cutting parameter when the material is anisotropic or/and non homogenous, like the material of this study. The cutting direction was quantified as an angle, θ , and consists on the angle between the cutting direction itself and a predefined main direction along the top layer fibers.

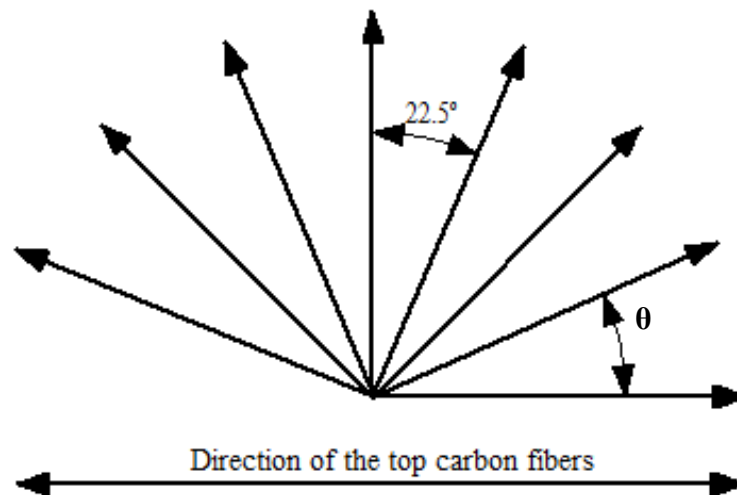


Figure 8. Cutting direction used on the present work. The 0° direction corresponds to cutting along the direction of the top layer fibers.

The experiments were conducted in 8 directions, as represented in Figure 8: 0° , 22.5° , 45° , 67.5° , 90° , 112.5° , 135° and 157.5° . This way cuts were made along the fibers, perpendicular to the fibers and in six intermediate directions.

3.6.1.2. Traverse speed

In order to choose the different traverse speeds for this work, some preliminary tests were made, taking into account the recommended values given by the OMAX software. The software has a scale of quality from 1 to 5, 1 corresponding to the fastest traverse rate and 5 to the slowest, for a given material and thickness. According to the manual of the machine software, quality 3 is considered to have the best speed/quality ratio.

So the first cut was made with quality 2 which corresponds to a traverse speed of approximately 3000 mm/min for a carbon fiber composite 4.4 mm thick. In these preliminary tests some flaws appeared on the surface faced to the nozzle and some waviness was present on the bottom of the cut.

Since the waviness increases with the increase of the traverse speed, it was decided that for general applications is not admissible to have a worse cut quality than the obtained, so only slower speeds were considered. Therefore, the used traverse speeds for this study were: 2000 mm/min (quality 3), 1500 mm/min (quality 4), 1000 (quality 5) and 500 mm/min.

3.6.1.3. Constant parameters

Some of the machining parameters were kept constant during the experimental work, like the:

- *Nozzle dimensions*: orifice diameter, focusing tube length and diameter;
- *Stand-off distance*. As shown before, it affects negatively the waterjet cutting process, so it should be as small as possible. The value of 1.5 mm (recommended by OMAX) shown to be the best choice since smaller distances often allowed the rebound of the waterjet in the workpiece to re-enter the nozzle, stopping the water stream and clogging the abrasive feed line;
- *Abrasive flow rate*;
- *Impact angle*. The tilting ability was not used, so the striking angle was the same in all cuts:

A resume of all the used operating parameters during this works, as well as the nozzle main dimensions, is made in Table 4.

Table 4. Design of experimental parameters for the cutting process.

Traverse speed [mm/min]	500, 1000, 1500, 2000
Cutting orientation - θ	0°, 22.5°, 45°, 67.5°, 90°, 112.5°, 135°, 157.5°
Water pressure [kpsi / MPa]	55 / 380
Stand-off distance [mm]	1.5
Abrasive flow rate [g/min]	350
Striking angle - φ	90°
Mixing tube diameter [mm]	0.762
Jewel diameter [mm]	0.3302

3.6.2. Cut design

Two main designs (shown in Figure 9 and Figure 10) were made to fit the purposes of the present work: type A, suitable for measuring the surface roughness and kerf taper angle and type B for measuring the kerf width and observe defects at the entry and exit points of the jet. All the cuts were designed bearing in mind the same principles: doing the least cuts, ease fixture for the measurements, and fitting to the selected operation parameters.

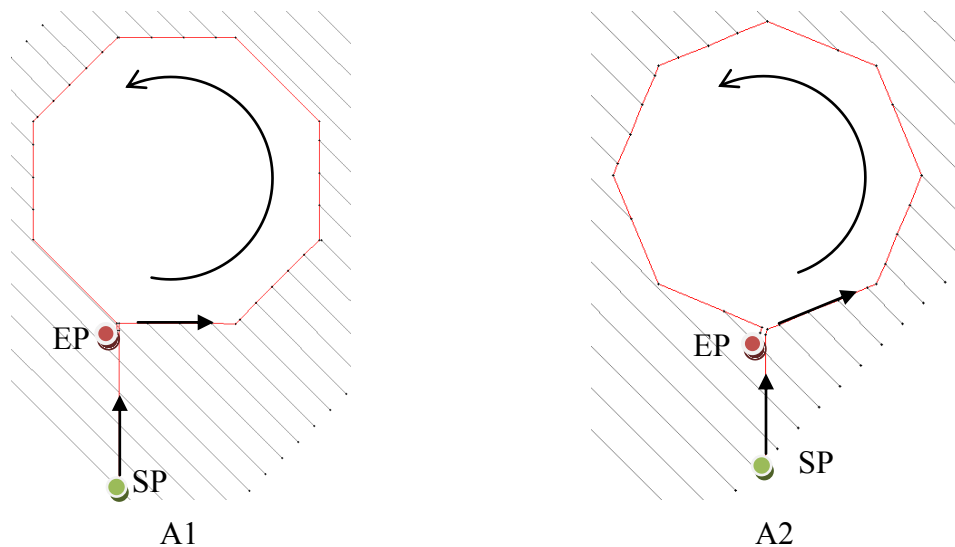


Figure 9. Type A cuts. These cuts were made in order to measure the surface roughness and the kerf taper angle variation with cutting direction. The A1 cuts focus in 0°, 45°, 90° and 135°, while the A2 cuts focus in the 22.5°, 67.5°, 112.5° and 157.5° cutting directions. SP and EP stand for, respectively, Start Point and End Point of the tool path.

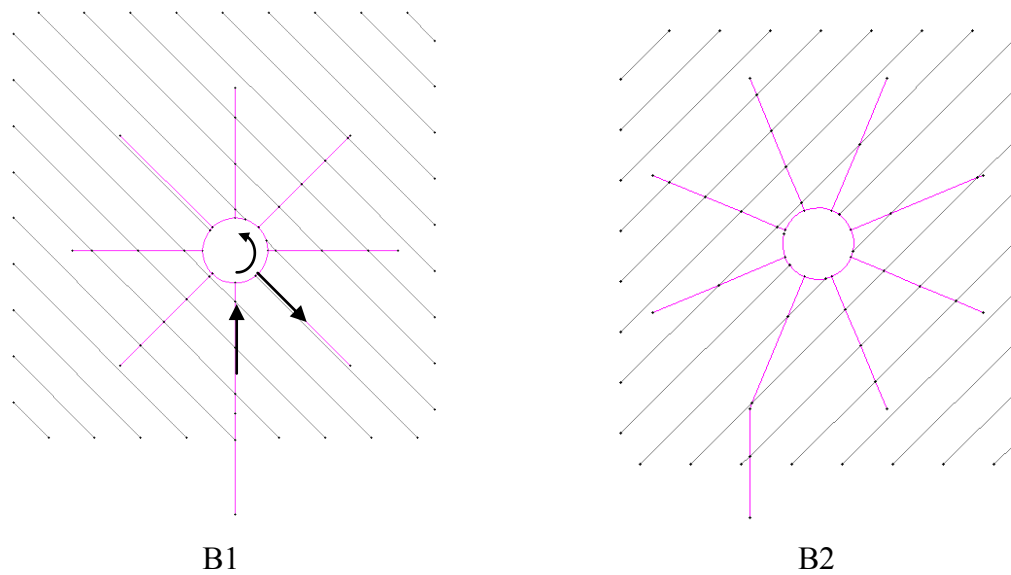


Figure 10. Type B cuts. These cuts were made in order to measure the top kerf width variation with the cutting direction. The presence and magnitude of minor defects such as surface chipping were also analyzed. The B1 cuts focus in 0° , 45° , 90° and 135° , while the B2 cuts focus in the 22.5° , 67.5° , 112.5° and 157.5° cutting directions.

3.6.2.1. Type A

The A cuts consisted on octagonal shapes with a side length of 25 mm, with two orientations in relation to the top layer fibers orientation, rotated to each other by 22.5 degrees.

This geometric shape was chosen because it has parallel sides making it easier to ensure the horizontality of the surface to the probe during the roughness measuring. Also it has the necessary room in the interior of the octagons where three holes were drilled after the cut, which were part of the fixture system created to measure the kerf angle at the Coordinate Measuring Machine (CMM).

With the A1 orientation the measured cutting directions were 0° , 45° , 90° and 135° , while with the A2 orientation were 22.5° , 67.5° , 112.5° and 157.5° .

In order to avoid the drop of the cut specimens into the water tank a tab was included, with 2 mm length and 0.5 mm width. A total of 8 specimens of this cut type were made with 4 different speeds in the two orientations.

3.6.2.2. Type B

The chosen geometry for the type B cuts was especially useful because it avoids the separation of the cut parts, which was a necessary condition in order to measure

the kerf width at the microscope. As in the type A cuts, there were two orientations: B1 and B2, rotated 22.5° to each other.

The length of the cuts for each direction was 30 mm length. No tabs were needed since the cut design did not include any closed contour, and therefore no separation of material from the main plate.

3.7. Measurements

3.7.1. Roughness

The measurements were conducted on a Taylor-Hobson machine, model Talysurf 4. The stylus was made of diamond and the tip (when new) had a width of 0.0025 mm. This machine only measured the average roughness R_a , expressed in micrometers in this work, and therefore was the chosen parameter to characterize the surface quality with regard to its roughness. A cut-off length of 0.8 mm was used, which led to a sampling length of 4 mm (5 times the cut-off length).

The roughness was measured at the middle of the kerf walls and at a distance of 1.2 mm from the middle, both up and down, as shown in Figure 11. The measurements were not made in the areas located immediately after the jet entry point and before the jet exit point to avoid measuring possible defects due to jet entry and exit.

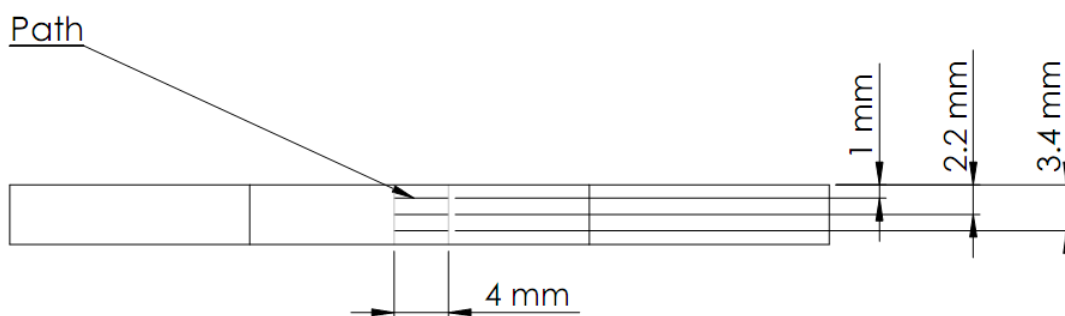


Figure 11. Schematic view of the sampling length (path) for the 3 kerf wall depths.

3.7.2. Kerf taper angle

The kerf taper angle was measured with a Zeiss West Germany CMM, model PMC V850. The software used to control and acquire data was the Calypso V5.0. The used stylus had a measuring spherical head with 2 mm diameter.

The type A samples were used for this purpose and in order to provide the required fixing for the measurements three holes were drilled as shown in Figure 12.a. In the middle hole a screw was tightened, which ensured the fixture of the sample to an aluminum support, while the other two holes were slot for two guide pins fixed at the mentioned support in order to guarantee the same sample orientation in all the measurements (Figure 12.b). The aluminum support was then clamped to a steel support that was bolt tightened to the machine. With the referred fixture system (Figure 12.c) it was possible to create a measuring plan within the CMM software, saving time while assuring that the same surfaces were being measured in all the samples.

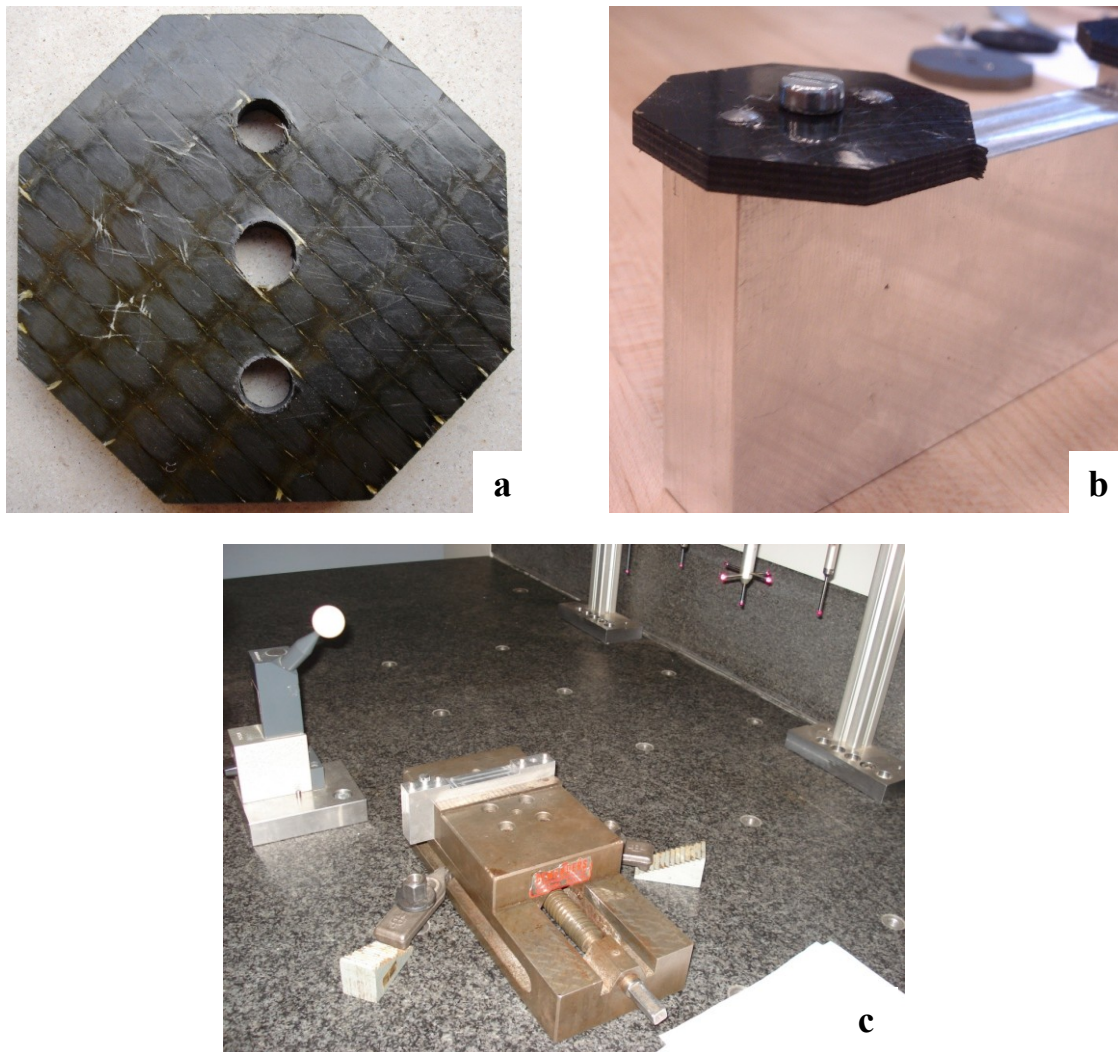


Figure 12. Fixation system used to measure the kerf angle of the cut: a – detail of the fixation holes drilled on the samples; b – sample fixed to the aluminum support; c – fixation system bolted to the CMM.

In order to know the kerf taper angle, a virtual plane was created by approximation to the points measured at the cut surface. To measure these points some spots were defined on the cut surface, which allowed the software to create a path. This path was then traversed by the stylus while taking coordinates each 0.1 mm of travel. Since samples had an octagon shape, the kerf taper angle was considered to be half the angle between the virtual planes of each two parallel cut faces.

Despite that not the entire generated kerf wall was suitable for measuring, because the used waterjet machine automatically decreases the traverse speed when approaching corners or small radius curves in order to avoid geometric distortions at the bottom caused by the jet lag. So the points were only measured on a 1.5 cm width zone at the center of each kerf wall, as seen in Figure 13, which corresponds to the cut zone where the nozzle traversed at the desired speed. This speed reduction effect was most noticeable for the higher traverse speeds, but in order to create an homogeneous procedure through all the measurements the worst case scenario was assumed.

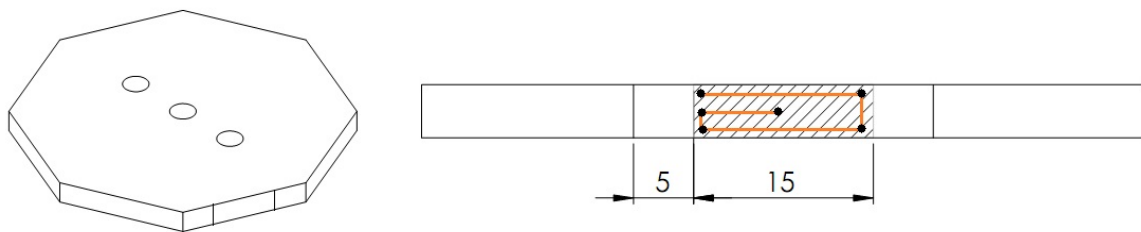


Figure 13. Zone suitable for kerf taper angle measurement, represented by the black and white striped pattern. The orange line represents the path taken by the CMM and the black dots the points that led to this path.

3.7.3. Kerf width

The top kerf width of the cuts was measured using an optical microscope connected to a computer. Three measurements were made at the entry point of the jet. The kerf width value was assumed to be the arithmetic mean of these 3 measurements.

The bottom kerf width was calculated from the equation:

$$K_{W,B} = K_{W,T} - 1000 \times h \times \tan(K_T) \quad [\mu m] \quad (1)$$

, being $K_{W,T}$ the top kerf width in μm , K_T the kerf taper angle in degrees and h the plate thickness in millimeters.

3.7.4. Waviness

The waviness of a given surface can be isolated from the surface profile, which is normally obtained by a machine as the one used on the present study to measure the surface roughness. However, such isolation is normally made through the use of mathematical tools, and once the used machine did not have a digital output this kind of analysis turned out to be impossible.

However, as mentioned in Chapter 2, the waviness only prevails in the deformation wear zone. Since the deformation wear zone only occur in certain conditions, the kerf walls were analyzed in search of the transition between the mentioned deformation wear and the cutting wear zone. When found, the depth of the transition was measured, and when not found it was considered that the cuts were waviness free.

3.7.5. Chain of procedures

Both the roughness and the kerf taper angle measurements were made using contact methods. Since they were made in the same samples, a chain of procedures was created in order to avoid or at least reduce the measuring of defects caused by the previous procedure.

Upon the surface roughness measuring some scratches may be created, since the stylus is very sharp and harder than the workpiece material. In the other hand, some scratches may be created during the drilling of the samples and the kerf angle measurement. However, the value of the roughness is around microns so it is more likely to have measurement errors due to scratches than the measured kerf taper angles by the CMM, which is only sensible to tens of microns. Therefore the roughness was measured first, as shown in Figure 28 of the Appendix B.

It was only important to create this chain of procedures to the type A cuts, since the type B cuts were not submitted to any procedures likely to have impact on the measured results.

4. RESULTS AND DISCUSSION

This chapter presents the results obtained with the described measuring methodology and the flaws that were created during the experimental cuts. A brief description of the problems encountered during the AWJM is also made as well as the solutions taken to overcome these problems.

4.1. Surface quality

As mentioned before, the surface quality depends on two main parameters: the surface roughness and waviness.

4.1.1. Waviness

After analyzing the kerf walls of the performed cuts, it was found that the transition between the smooth cutting zone (cutting wear zone) and the rough cutting zone (deformation wear zone), which is referred to have waviness as the main defect, only occurred in the cuts performed at the speeds of 2000 mm/min (Figure 14.b) and 1500 mm/min (Figure 14.c). With the speed of 1500 mm/min the transition occurred almost at the end of the kerf wall, at approximately 4 mm deep. In the other speeds the trail left by waterjet was completely straight.

Comparing the kerf walls created on a steel plate (Figure 14.a) with the ones created in the studied composite, it is possible to see that the mentioned transition is not perfectly visible in carbon fiber. This is because the surface quality drop with the cut depth, observed in the steel cuts, is not noticed in the performed cuts. In fact, the transition was only identified by the direction change of the trail left behind by the waterjet passage

So, in order to know the actual state of the surface with regard to the surface waviness, further measurements should be made with a digital profile meter, or other equipment able to give information about this parameter.

No relationship between the cutting orientation and the transition depth was found.

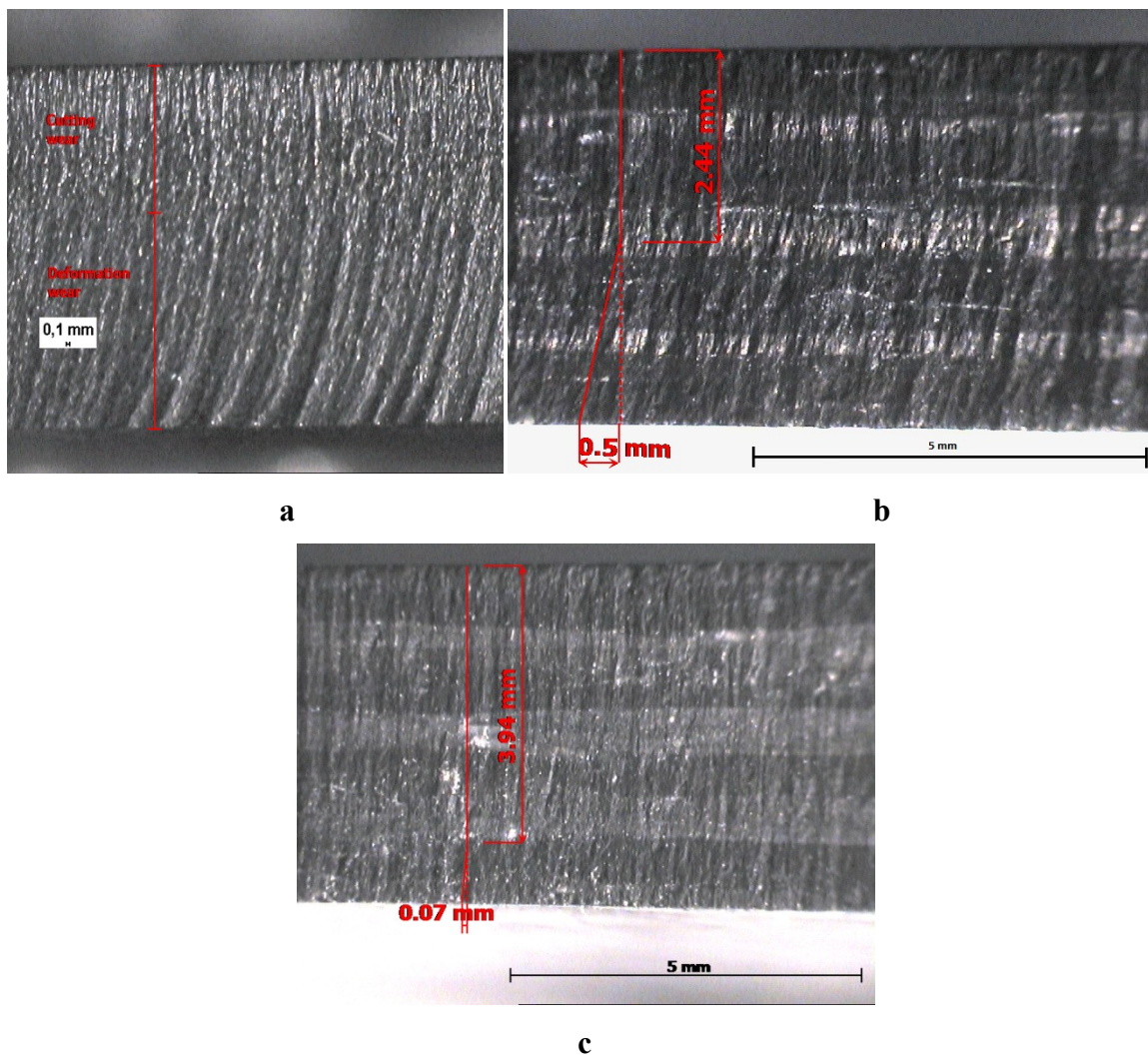


Figure 14. Transition between the smooth cutting zone (cutting wear zone) and the rough cutting zone which presents waviness: a – Rst 37.2 (DIN 17100) steel 6 mm thick cut at a traverse speed of 500 mm/min (retrieved from the work made by Dias, 2011); b – carbon fiber cut at 2000 mm/min with a cutting orientation of 45°; c - carbon fiber cut at 1500 mm/min with a cutting orientation of 45°.

4.1.2. Surface roughness

The variation of the measured R_a values with the cutting orientation and depth, for the tested traverse speeds, is shown in the graphics of Figure 15.

The cutting direction of 90° showed the greatest R_a for the traverse speeds of 2000, 1500 and 1000 mm/min, for all the cut depths, except for the cut depth of 1 mm at a traverse speed of 1000 mm/min, where the R_a value for $\theta = 22.5^\circ$ was the highest.

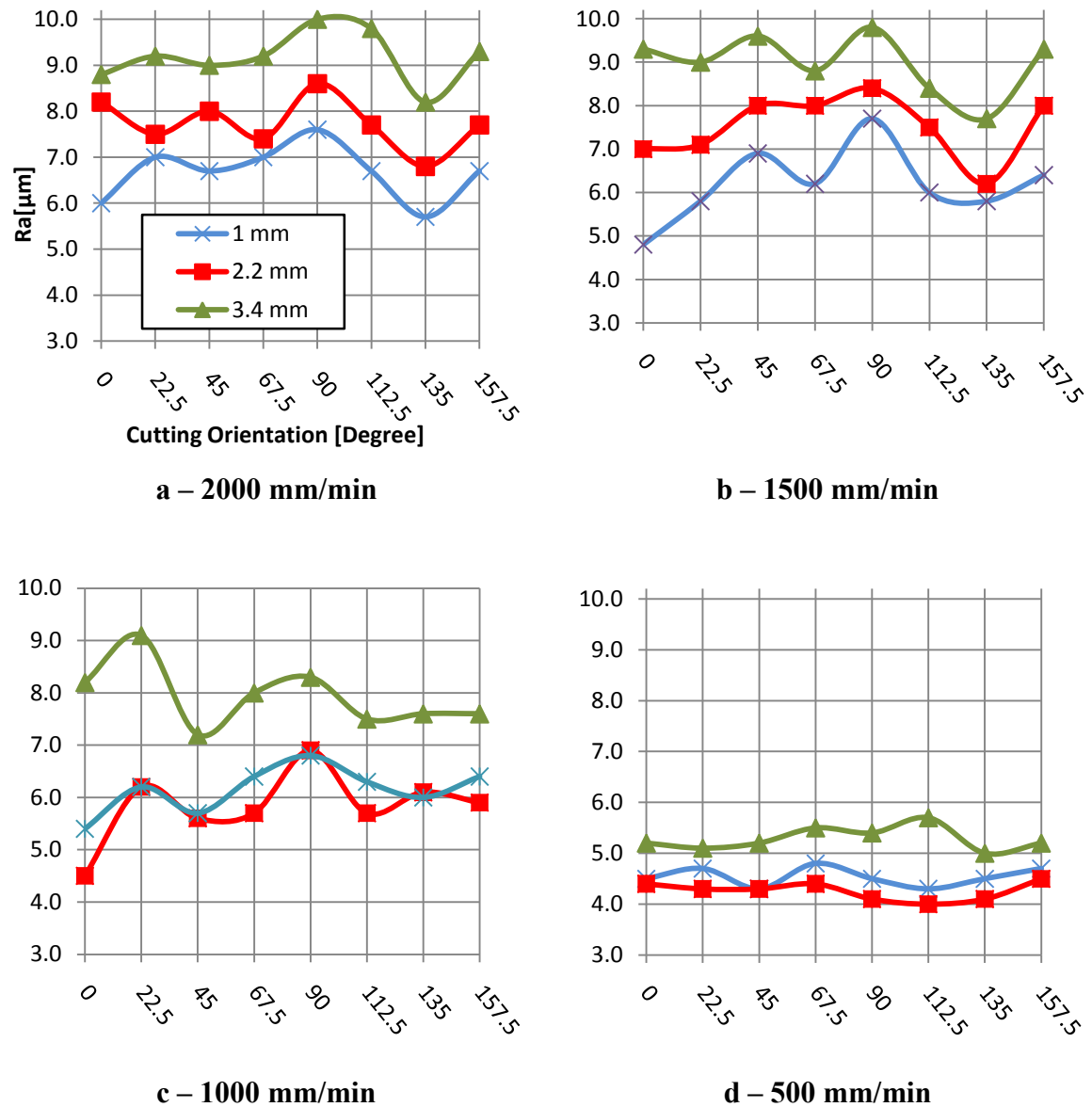


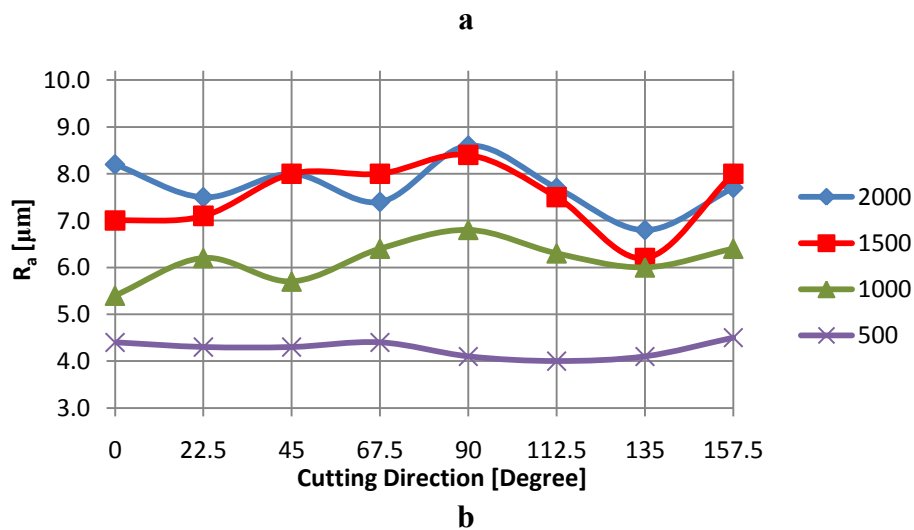
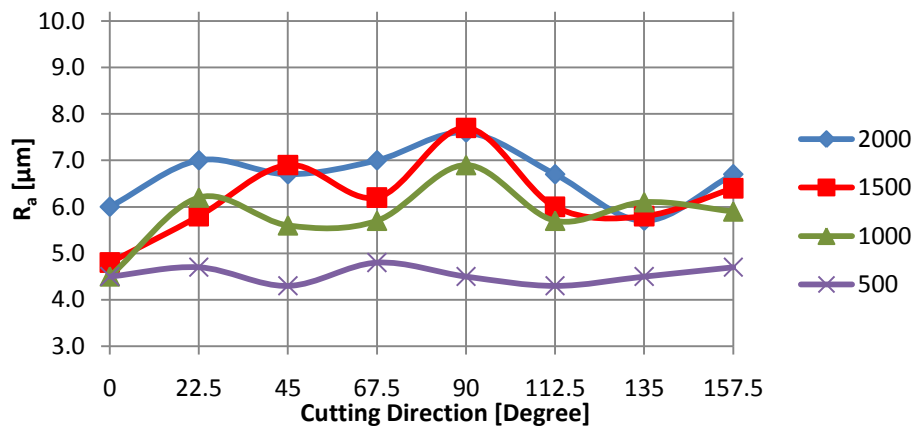
Figure 15. Roughness variation with the cutting direction and cut depth, at the four different traverse speeds: a – 2000 mm/min; b – 1500 mm/min; c – 1000 mm/min; d – 500 mm/min.

The surface roughness depends greatly of the kinetic energy present on the abrasive particles within the waterjet and the number of these particles that hit the kerf wall. However, even if there are lots of particles, if they do not have enough speed they will not effectively erode the surface. Therefore, when cutting perpendicular to the fibers ($\theta = 90^\circ$) the amount of energy dissipated at the top layer can be higher than when cutting in other directions, which leads to lower particle speed increasing the R_a values along the kerf wall. Nevertheless repeatability tests should be made to confirm this trend and the R_a value peak for the cut made with $\theta = 22.5^\circ$ at a traverse speed of 1000 mm/min.

For the traverse speed of 500 mm/min the variation of the R_a value with the cutting direction was rather small and therefore no relation was found between them. This can be justified with the increased kinetic energy of the waterjet along the cut depth, due to the lowest traverse speed, which leads to less sensitivity to the orientation of the top layer carbon fibers.

The variation of the measured R_a values with the cutting orientation and the traverse speed, for the 3 measured cut depths, is shown in the graphics of Figure 16. It is visible in all the graphics that the cut speed of 500 mm/min, as mentioned before, shows insignificant variation with the cutting direction, as well as the lowest R_a values.

Therefore it seems that there is a critical value for the traverse speed, somewhere between 500 and 1000 mm/min, where values below this one allows the jet to create smoother surfaces, with similar R_a values for all the cutting directions. This may be because below this value the mentioned energy loss due to the cut orientation is lower than the increase of the energy due to the decrease of the traverse speed.



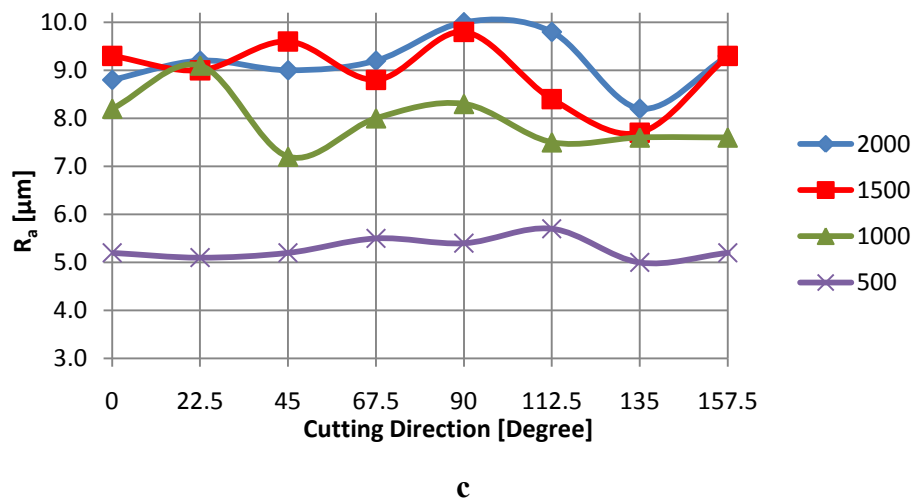


Figure 16. Roughness variation with the cutting direction and traverse speed, for the three different cut depths: a – 1 mm; b – 2.2 mm; c – 3.5 mm.

If the average values of the measured surface roughness for each surface depth and each traverse speed are analyzed (which is the same as ignoring the cut orientation as an operation parameter), as seen in Figure 17, it is possible to ascertain that the roughness increases with the cut depth for the speeds of 2000, 1500 and 1000 mm/min. Although, when cutting at a speed of 500 mm/min, the surface roughness decreased from the top (1 mm) to the middle (2.2 mm) and then raised again at the bottom (3.4 mm). This may be due to greater jet stability at the cut depth of 2.2 mm. Nevertheless, cuts with thicker plates should be made to understand this behavior.

It is also noticeable that the surface roughness decreased with the traverse speed (Figure 17), which was already expected, given the obtained results on the studies developed by Ramulu *et al.* (2009) and Akkurt *et al.* (2004). Such behavior is possibly due to the higher number of abrasive particles hitting the kerf walls at slower speeds, combined with more kinetic energy which gives to the surface a smoother finish. However, the rate of roughness decrease was not the same for all the cut depths and not even equal between the cut speeds. For example, at a cut depth of 2.2 mm, a reduction of the cut speed from 2000 to 1500 mm/min (25%) resulted in a decrease of the average R_a of about 2.7%, while a reduction from 1000 to 500 mm/min resulted in a decrease of about 30.7%.

The measured values of roughness may have some inaccuracy (beside to the associated to process uncontrollable variations and measurement equipment) since the positioning of the samples were made by hand, and, as seen in Figure 14.c, the layers were

not completely defined or even aligned with the path of the roughness meter, which can create variations on the measurements through the different cut conditions.

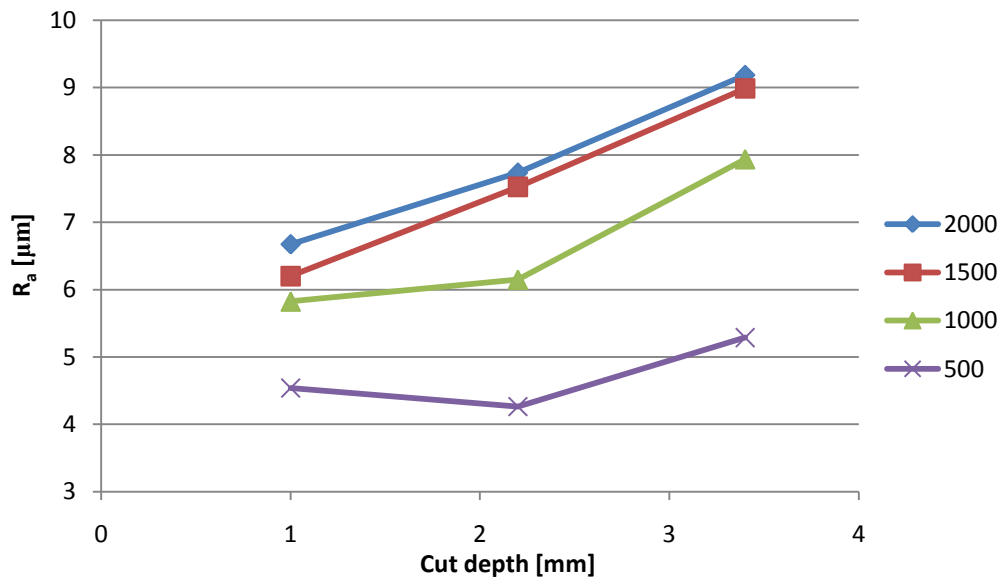


Figure 17. Variation of the average values of R_a with the traverse speed [mm/min] and the cut depth.

Although the used roughness parameter (the average roughness R_a) is one of the most used parameters, it is an average value, so it only detects general variations in overall profile height, and defects in the surface do not have great influence on the measurement. Also, two different profiles can have similar R_a values, since this parameter does not make distinction between peaks and valleys. Therefore the measured values do not give a full characterization of the surface profile.

4.2. Kerf taper angle

The variation of the measured kerf taper angle with both the cutting angle and traverse speed is shown in Figure 18. The cutting direction of 45° showed a tendency to have the greatest values of taper for all cut speeds, apart from the traverse rate of 1000 mm/min, where the cutting direction of 135° presented a similar value. In fact, the cutting directions of 0° and 135° also showed greater values than the average for the speeds of, respectively, 1500 and 1000 mm/min, and 1000 and 500 mm/min. In order to ascertain the real effect of the cutting orientation on the kerf taper angle, repeatability tests should have been made to confirm the mentioned trends.

All the measured angles were positive, so the critical speed that allows taper free cutting ($u_{c,T}$) is lower than 500 mm/min. According to the OMAX software this critical speed is approximately 76 mm/min for a generic carbon fiber laminate composite with a thickness of 4.4 mm.

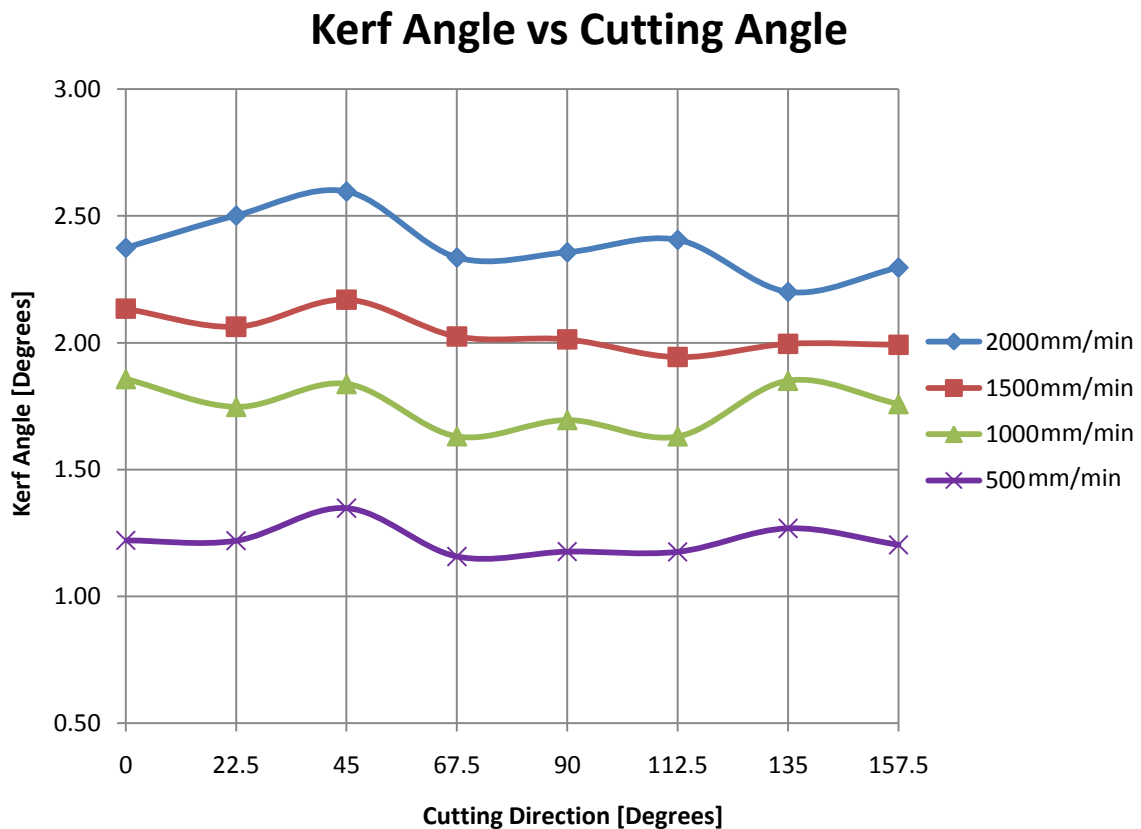


Figure 18. Kerf taper angle variation with the cutting orientation and traverse speed. Traverse speed in mm/min.

Although there are differences between the kerf taper values for the different cutting orientations, the range of values is small, and tends to be even smaller with the decrease of traverse speed, as seen in Table 9, of Appendix D. So the greatest range of values was obtained with the cut made at 2000 mm/min with a value of 0.4 degrees, which means a 0.03 mm variation of the bottom kerf width through the cuts with different cutting orientation.

For the used thickness the taper variation had little effect on the bottom kerf width dimensions, but if cutting a thicker workpiece, for example 15 mm, and assuming that the taper angle is not dependent on the workpiece thickness, a taper variation of 0.4 degrees means a bottom kerf width variation of 0.13 mm.

As expected, increasing the traverse speed also increased the kerf taper angle. Higher traverse speed leads to a smaller exposure time which allows less jet overlapping on the kerf walls, causing a greater kerf taper angle, as explained on the work developed by Shanmugam and Massod (2009).

This relation between the traverse speed and the kerf taper angle is similar to the one obtained in the study made by Shanmugam and Masood (2009) with carbon fiber and different from the one obtained by Wang (1999) with a Teflon/Phenolic resin composite. Maybe the cut material used in the Wang (1999) study has a very high machinability, which allows the effective jet diameter to keep up with the traverse speed increase, leading to low sensitivity of the kerf taper angle to this parameter. Further testing in Teflon/Phenolic resin materials should be made at slower speeds than 1000 mm/min to confirm this assumption.

If in a certain cut the kerf taper angle is being corrected by tilting the waterjet nozzle, some problems may occur due to the effect of the traverse speed on the kerf angle. For example, if the nominal speed for a given cut is 2000 mm/min, the nozzle should be tilted approximately 2.38° in order to obtain a taper free workpiece. However, during the cutting the nozzle may need to slowdown which, according to the obtained results, reduces the kerf taper. Since the cut is now taper free (kerf taper angle ≈ 0) any decrease in the traverse speed will lead to negative values of taper. Therefore if high precision is required it might be needed to set the tilting compensation separately along the tool path depending on the traverse speed at a given point.

According to the study made by Shanmugan *et al.* (2008), delamination on layered composites is caused mainly by water wedging. When using tilting compensation the waterjet hits the layers lengthwise, so the water wedging phenomenon might be enhanced. Therefore further studies should be made to ascertain the effectiveness of this taper correction technique on carbon fiber as well as its influence on delamination.

4.3. Kerf width

The results from the top kerf width measurements, as well as the range of the values for each traverse speed are shown in Table 5. The reason why the average was also calculated is explained later. Only the results for $\theta = [0^\circ; 45^\circ; 90^\circ; 135^\circ]$ are shown due to the lack of time to measure the values for the other cutting directions.

Table 5. Top kerf width values obtained from the microscope measurements. Kerf width values in microns.

<i>Top Kerf</i>	Traverse Speed [mm/min]			
Cutting Orientation	2000	1500	1000	500
0°	754	768	797	830
45°	762	786	808	838
90°	759	776	804	830
135°	745	764	792	825
Range	17	22	17	13
Average	755	773	800	831

The variation of the top kerf width values with the cutting orientation is rather reduced, having the maximum value of 22 μm for a traverse speed of 1500 mm/min.

The bottom kerf width was calculated using equation 1, which takes into account the top kerf width value, the kerf taper angle and the plate thickness.

Table 6. Bottom kerf width values calculated from the top kerf width measurements and kerf taper angle measurements. Kerf width values in microns.

<i>Bottom Kerf</i>	Traverse Speed [mm/min]			
Cutting Orientation	2000	1500	1000	500
0°	572	604	655	736
45°	562	619	667	734
90°	578	621	673	739
135°	576	610	650	728
Range	16	17	23	11
Average	572	614	661	734

Like the measured top kerf values, the bottom kerf width had almost no variation with the cutting orientation, having the maximum value of 23 μm for a traverse speed of 1000 mm/min. These variations are far too small to relate them with the cutting orientation since there are other variables that can cause that amount of variation, such as the inaccuracy associated to the measurement by itself. This inaccuracy is especially

important because the measurements depended directly from the human eye and personal judgment.

So it is possible to say that the cutting orientation had little or no influence on the kerf width values. Therefore the cutting direction parameter was discarded, and the kerf width for each traverse speed was considered to be the arithmetic mean of the kerf width values for all the different cutting directions.

As shown in Figure 19, the kerf width increases with the decrease of the traverse speed. This might be because at slower speeds the jet overlapping is higher, which allows more abrasives to hit the kerf walls and therefore removing larger amounts of material. This model is proposed by other works like the one made by Wang (1999).

In order to know the maximum kerf width the machine was programmed to hold 3 seconds with the waterjet turned on at the end of the tool path. This way it was guaranteed that the profile of the kerf wall at those points followed the waterjet effective profile. The maximum top kerf width for the used operation parameters was 1 mm and it is represented in Figure 20. This value is also the effective diameter of the jet at the distance of 1.5 mm from the nozzle.

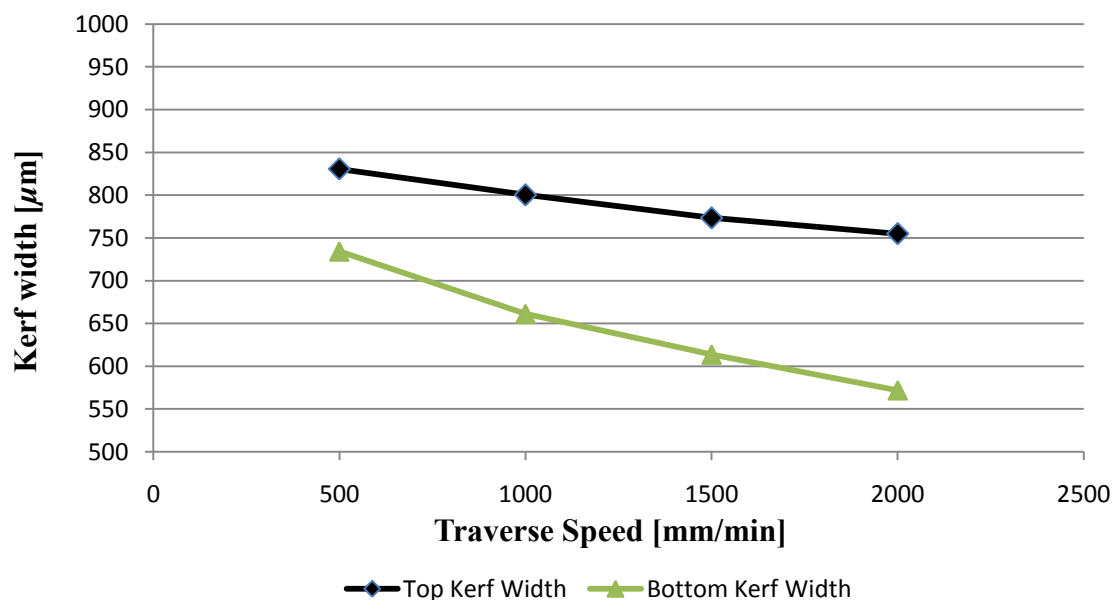


Figure 19. Kerf width variation with the traverse speed: black line – top kerf width; green line – bottom kerf width.

In order to avoid geometrical distortions from the jet lag during the AWJM, it is required to reduce the traverse speed when cutting small radius curves (or other geometries susceptible to these kind of flaws, like corners) and during the approach to the

tool path end. Since the kerf width increases with the traverse speed decrement it might be needed to have a dynamic value for the tool offset value in order to obtain high precision cuts. Considering the used operation parameters and material, if it was required at some point of the cut the reduction of the traverse speed from 2000 *mm/min* to 500 *mm/min*, errors of approximately 0.038 mm and 0.081 mm, respectively at the top and bottom, would be committed. Although it is not much, if not avoided this effect can compromise the cut when tight tolerances are required. Normally this effect is less significant when cutting at slower speeds since the speed differences are smaller, as may be seen comparing Figure 20.a and Figure 20.b.

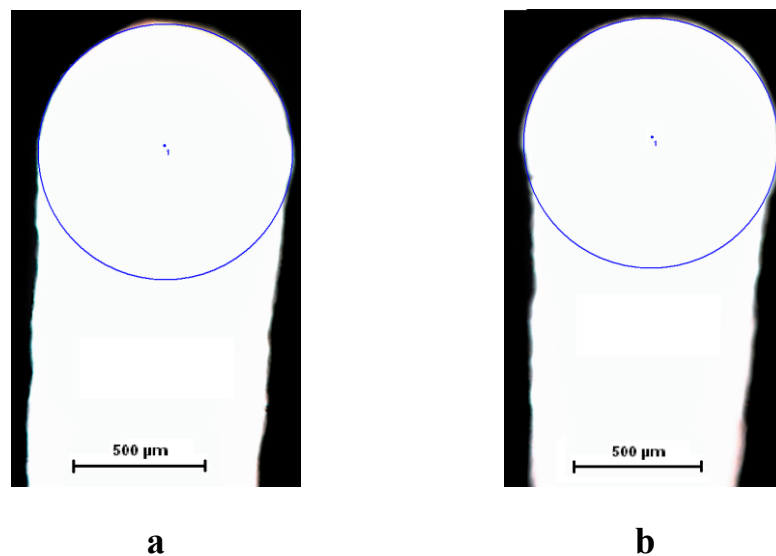


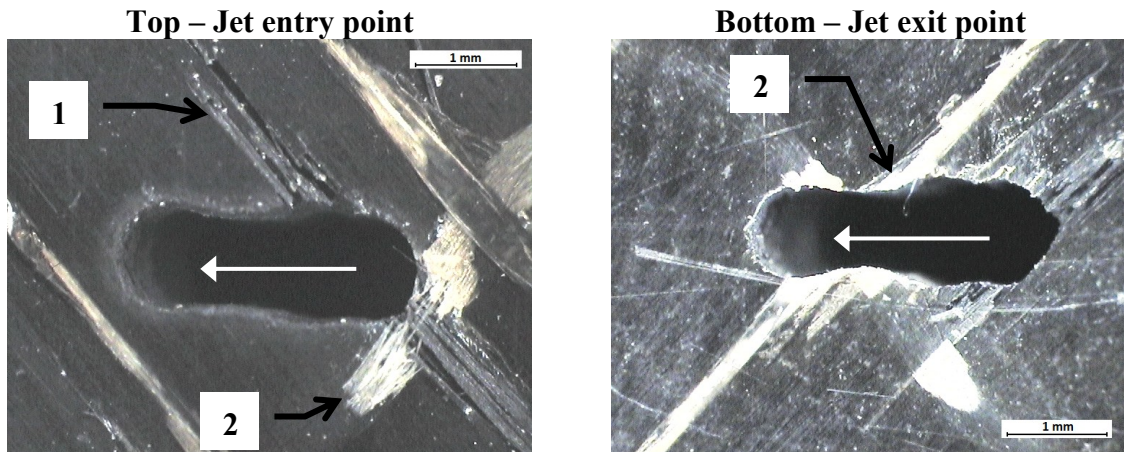
Figure 20. Slowing down effect on the top kerf width and maximum kerf width measurement at a rated traverse speed: a – 500 *mm/min*; b – 2000 *mm/min*. Pictures taken using an optical microscope with a digital camera connected to a computer with a magnification of 10X.

4.4. Piercing testing

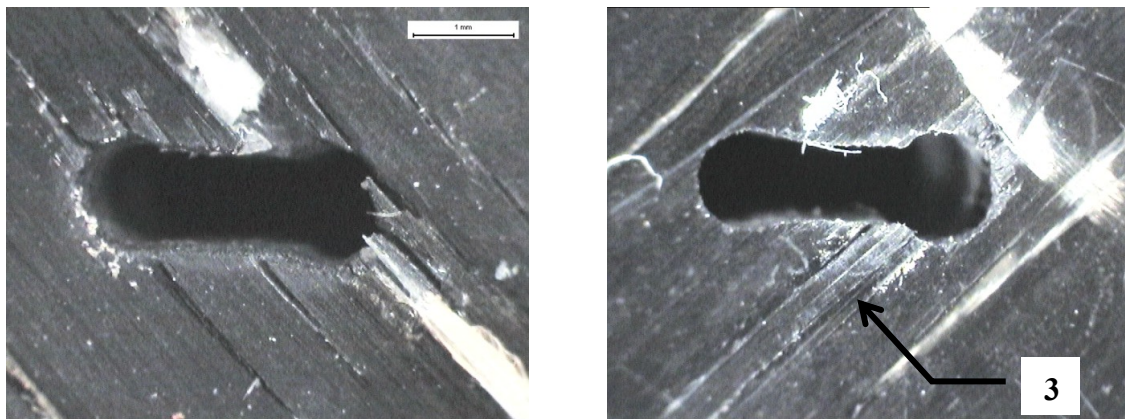
It was not possible to measure the extent of the damages in the inside of the material, so only the damage visible at the surface was analyzed. The non-destructive methods commonly used to check for defects inside carbon fiber composites are the ultrasonic testing and x-ray (CT-Scan). The damage at the plate surface, caused by the piercing methods, was mainly delamination of the upper layers of the composite and pullout of the polyamide and glass fibers, as illustrated in Figure 21. The measured affected areas are shown in Table 8 of the Appendix C.

Among all the tested piercing methods, the ones that showed a larger affected

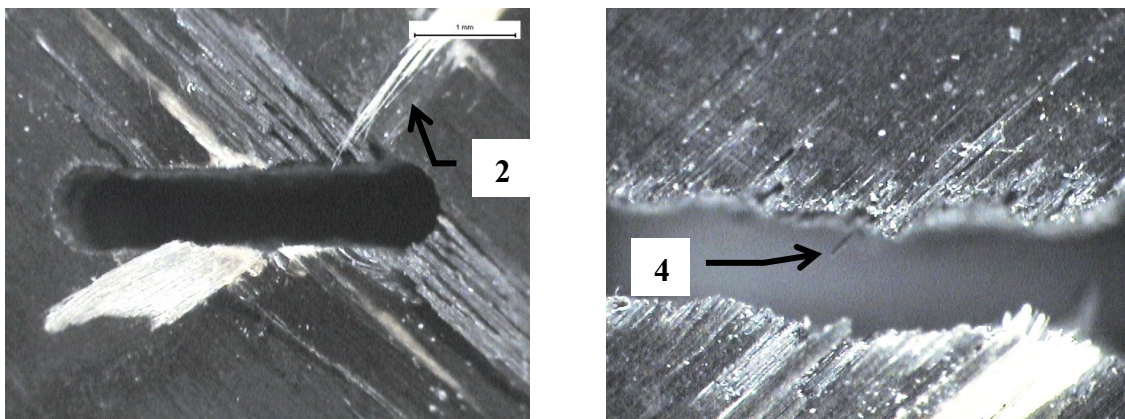
area at the entry point were the stationary piercing (Figure 21.d) and the water only dynamic piercing (Figure 21.c). The dynamic piercing at low pressure with the “brittle mode” showed the smaller affected area (Figure 21.a). At the exit point of the jet the affected area was similar in all the piercing methods. At the bottom the main defects were some cracks along the fibers of the last layer.



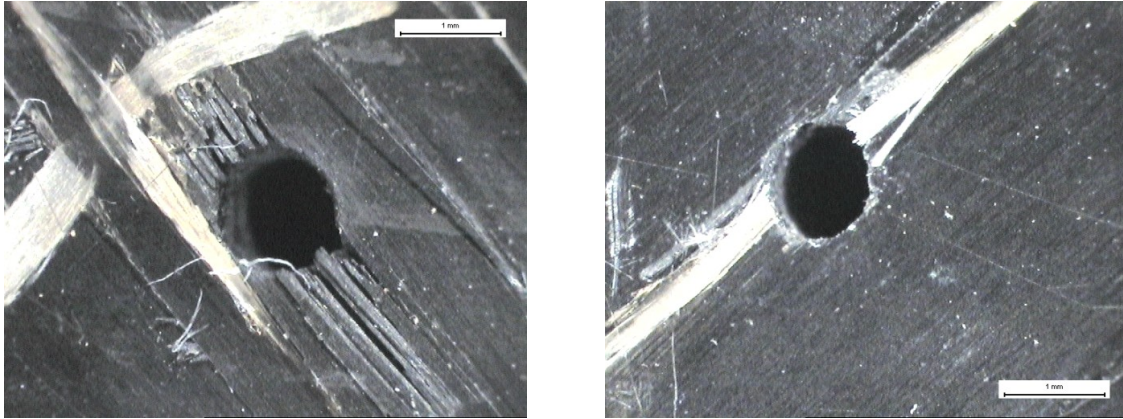
a) – low pressure dynamic piercing with “brittle mode” on



b) – Dynamic piercing



c) – Water only dynamic piercing



d) – Stationary piercing

Figure 21. Damage created by the tested piercing methods at the surface of the plate: 1 – Delaminate carbon fibers; 2 – Pullout of the polyamide/glass fibers; 3 – Carbon fiber cracking; 4 – uncut carbon fiber. The white arrows represent the direction of the piercing and are the same for all the dynamic piercing photos. Scale: 1 mm.

The shock wave impact of the waterjet seems to create a bullwhip effect on the fibers (Figure 21 identified as defect 1), which promoted a larger affected area along the directions of the top layer fibers. Therefore the affected area had an elliptical shape, instead of circular, in all of the tested piercing methods.

Since all the tested piercing methods failed to pierce without creating defects like cracking, fiber pullout and delamination, other solution was used to cut the specimens: start cutting outside of the plate. Other solution that could be used would be to drill a hole first and then start cutting from that hole, which would create similar conditions as starting the cut from the outside of the plate. Drilling systems attachable to the nozzle with full integration in the machining process are already available from different manufacturers.

4.5. Defects created during the experimental cuts

During the AWJM some defects appeared near the entry and exit points of the jet, such as cracks and fiber pullouts or uneven breaking of the glass and the polyamide fibers.

4.5.1. Surface Chipping

Although the surface cracks could be felt by sliding the fingertips in the surface they were scarcely visible, especially because their visibility greatly changed with the

slightest lighting conditions variation. Using a microscope to analyze these flaws proved to be a very time consuming method, because almost all the time was spent changing the light intensity and direction.

From the observation of the cuts it is possible to conclude that this phenomenon was affected by:

- *Traverse Speed* – with slowest speeds the crack length was smaller, as shown in Figure 22. No relationship was found with the number of cracks.
- *Cutting direction* – when cutting along the fibers ($\theta = 0^\circ$) there were no cracks while cutting perpendicular to the top layer fibers ($\theta = 90^\circ$) cracks with similar lengths appeared on both sides of the cut. With a cutting orientation of 22.5° , 45° or 67.5° the cracks occurred mainly on the right side of the cut while with 112.5° , 135° and 157.5° the cracks appeared mainly on the left side.

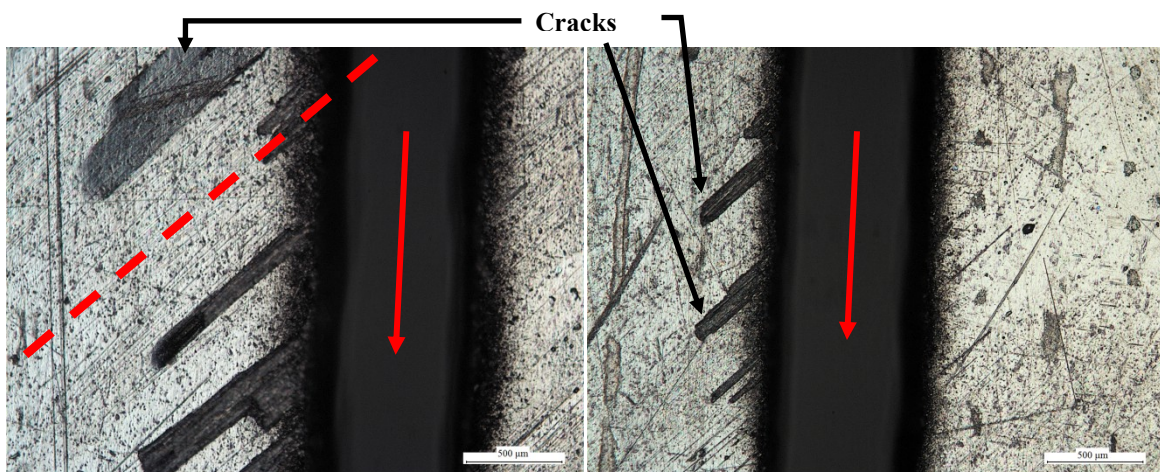


Figure 22. Surface chipping on the entry jet zone made by AWJ cutting. Cutting direction of 45° and traverse speed of: Left photo – 2000 mm/min; right photo – 1000 mm/min. The red arrow represents the cut direction and the dashed orange line the top layer fibers orientation. Photos taken with an optical microscope with a camera connected to a computer and a magnification of 10X. Scale: 500 μm .

Considering that the angles θ and β , shown in Figure 23, are the angles between the cutting direction and the orientation of the top layer fibers, respectively measured at the right and at the left side of the cutting direction, a set of conditions relating this two angle can be created in order to predict in which side of the cut cracking will occur. These conditions are resumed in Table 7.

Table 7. Conditions of the prediction rule for the surface chipping side. The chipping side refers to the right or left side when facing the cutting direction.

Condition	Chipping Side
$\theta < \beta$	Right
$\theta > \beta$	Left
$\theta = 0^\circ$	No cracks
$\theta = 90^\circ$	Both sides

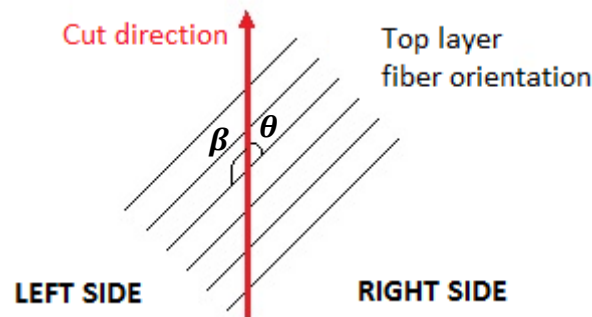


Figure 23. Angles between the cut direction and the fibers. With this cutting conditions surface chipping would occur mainly on the right side since $\theta < \beta$.

4.5.2. Fiber partially cut

In some cuts, the polyamide fibers were not totally cut, as shown in Figure 24. This phenomenon occurred only at the jet exit point and when cutting with a θ value of 45° and 135° , and only affected the polyamide fibers of the last layer.

It is known that the jet loses energy, and therefore speed, with the increase of the cut depth. Also the water jet exits by a focusing tube, and it is also known that in a flow within a tube the velocity of the fluid is lower on the outskirts of that flow. So this speed loss coupled with a lower speed at the periphery of the flow can be enough to allow the polyamide fibers to break in half and be dragged by the flow, rather than break upon the abrasive water jet impact near the kerf wall.

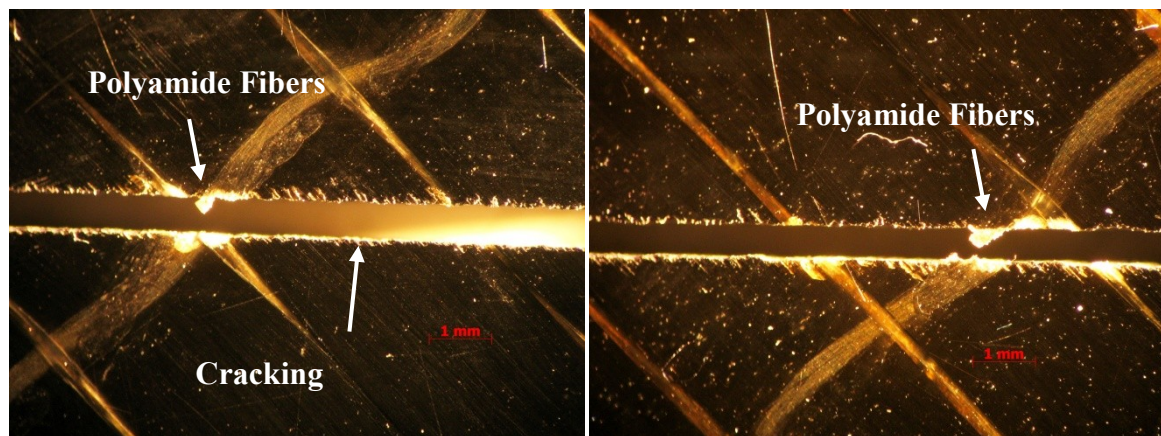


Figure 24. Flaws that occurred at the exit point: partially cut polyamide fibers and cracking. The left cut was made with a traverse speed of 500 mm/min and the right one at 1000 mm/min. Both cuts performed with $\theta = 45^\circ$.

The waviness of the polyamide fibers within the material, visible in Figure 24, was present before the cutting being created during the manufacturing process of the carbon fiber composite.

4.5.3. Cracking – Exit point

Cracks were found in all the cuts, next to the jet exit point, as shown in Figure 24. The used operation parameters, such as traverse speed and cut orientation, have showed no influence on the occurrence of this cracks.

The formation of these cracks can be explained by the lack of support of the carbon fiber of the last layer, which in combination with the lower energy of the jet at the exit point allows the fibers to bend instead of being cut by the waterjet. This bending action may be enough to crack the matrix material which creates the referred cracks.

4.5.4. Fiber pullout

Whenever machining with certain operation parameters, some fiber pullout occurred near the jet entry point. Only the glass and the polyamide fibers seem to suffer from this problem. This phenomenon was affected mainly by the cutting orientation and the eventual passing of the jet over crossings between the glass and the polyamide fibers of the top layer. These defects are shown in Figure 25.

Probably the glass fibers are shattered upon the waterjet contact, which is a known problem with very brittle materials. The polyamide fibers seem that are pulled out,

dragged with the water stream and eroded during the dragging. After the passage of the waterjet the polyamide fibers retract to its original position, but now they are shorter due to the eroding process.

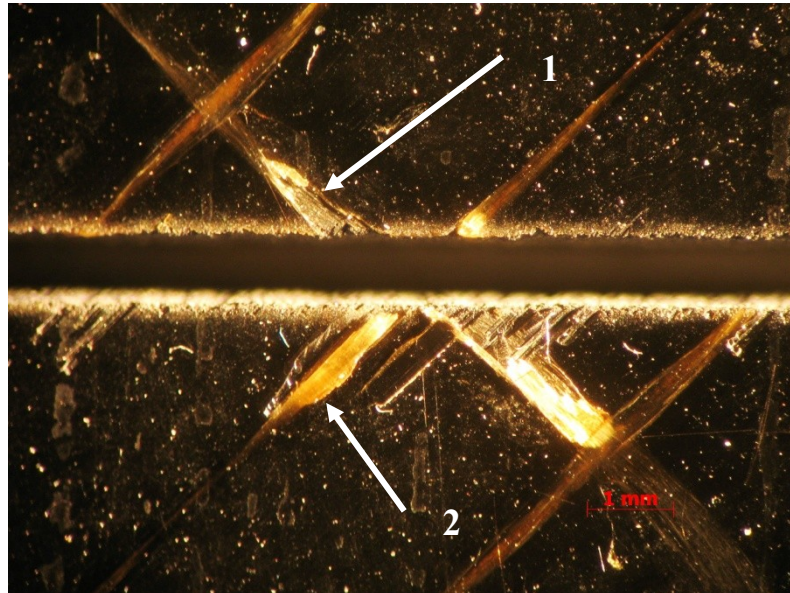


Figure 25. Flaws created near the entry jet point. Label: 1 – Polyamide fiber; 2 – Glass fiber.

4.6. Problems during the AWJC

During the AWJ cutting process some problems arose, some of them due to the process characteristics and others from the lack of knowledge and experience with the machine and the method. In order to fulfill the objectives of this study, these problems had to be solved and the taken solutions are presented beneath.

4.6.1. Workpiece fall into the water tank

The current standard in the waterjet process is to hold the material to cut on the top of supporting slats vertically aligned. Since these slats are normally underwater and subject to wear by the water jet, they are normally stainless steel plates due to its resistance to corrosion.

If the workpiece is smaller than the distance between slats there is a chance that it will fall into the water tank. To avoid this two solutions are normally used:

- *Replacement of the support slats by a waterjet brick*, which is a rectangular piece of corrugated plastic such as polypropylene. This solution has

associated costs (acquisition and replacement costs) and may reduce the productivity due to the high wear rate of the material. Also it fills the catch tank with gummy plastic powder which can clog the filters forcing their replacement or cleaning(www.waterjets.org);

- *Embedding a tab on the workpiece design.* Although not requiring the purchase of new materials, it might be needed to run some trials to know if the selected tab is strong enough to hold the workpiece. Also when cutting thick materials it proved to be hard to separate the workpiece, sometimes requiring post-processing to separate the tab and eliminating it from the workpiece.

Since no kind of waterjet brick was available during the current study, tabs were created during the workpiece design in order to avoid falling of specimens.

4.6.1.1. Tab testing

It was considered that if post-processing was required to separate the workpiece from the main plate some unwanted defects could be created on the specimens. So, some different tabs were tested in order to design a tab that had enough strength to hold the specimen and at the same time allowed the separation just by using hand force.

Tests with different gap lengths were made: 2, 1.5, 1 and 0.5 mm, while the leg length was kept constant at the value of 2 mm.

Despite all the tested tabs proved to be strong enough to avoid the specimens from falling into the catch tank, only the tabs with gap lengths smaller than 1.5 mm allowed separation using reasonable force. The gap length of 0.5 mm was selected since it provided the best ratio strength/easiness of separation.

4.6.2. Frosting and surface scratches

During the preliminary tests some frosting and surface scratches were observed as seen in Figure 26. The frosting is a result of the splash back of the water jet on the support slats. If the traverse speed is slow enough to allow long exposure times to the splash back, irregular gaps may appear at the bottom of the workpiece. The surface scratches are created at the interface workpiece/support slats due to high frequency

vibrations present during the process. The scratches are enhanced by the sharp shape of the slats (after some wear) and the abrasive particles “trapped” between them.

These are known problems associated with the process and normally they can be avoided using sacrificial materials at the bottom of the plate. Plywood was used as sacrificial material in the present work due to its high machinability, low cost and availability at the time of the cuts. While solving the referred problems, it turned out not to be the best choice since it absorbs high amounts of water in short periods of time. The water absorption caused dimensional variations on the plywood which made it impossible to guarantee the desired stand-off distance and the perpendicularity of the nozzle to the plate (striking angle $\varphi = 90^\circ$). This situation was confirmed with some inaccurate kerf taper angle measurements.

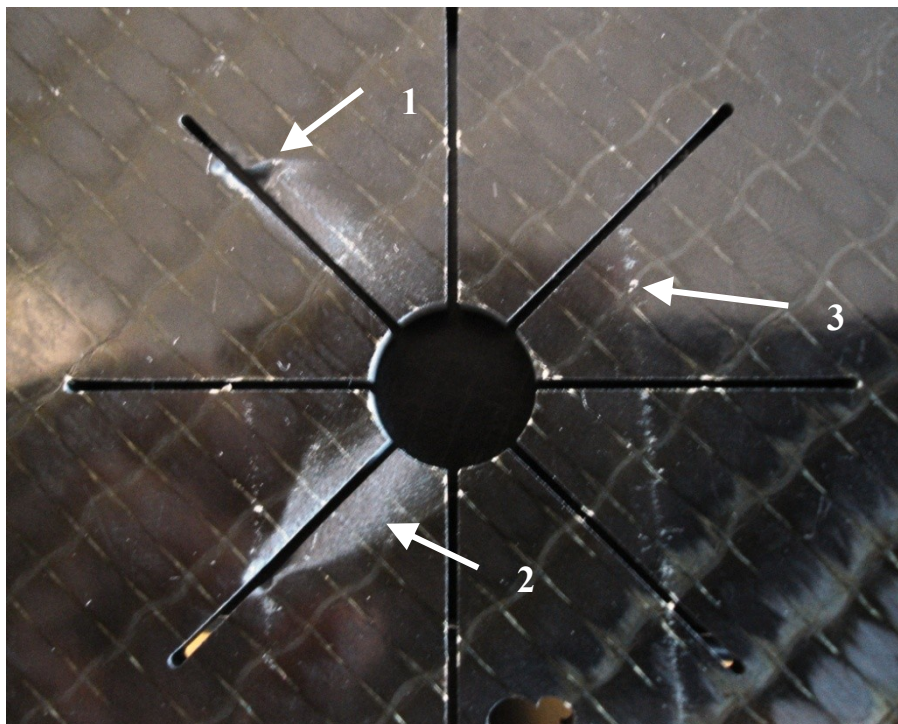


Figure 26. Defects created at the bottom of the plate during the AWJM at 500 mm/min: 1 – gap created by long exposure to the jet splash back; 2 – Frosting due to jet splash back on the support slats; 3 – scratches created at the support slats/plate interface.

So the adopted solution consisted in aligning the nozzle to a starting position where it would not traverse any support slat during the cut process. This was only possible because the specimens were smaller than the distance between the slats. Although this solution has shown to suit this study purposes, it can be difficult to apply on industry since

the alignment of the workpiece in the middle of the slats proved to be a time consuming procedure and it can even be impossible if the workpiece is larger than the distance between the slats.

The distance between the slats can be increased by removing one or more slats, but the increased gap between the supports might create some problems like bending and greater amplitude vibrations upon the AWJC. This is more likely to occur in thin plates and/or materials with low Young's modulus.

4.6.3. Geometrical defects

Geometrical defects like non circular holes (Figure 27) or bumps at the surface appeared in some cuts. In all of these cases the problem was caused by bad fixture of the plate, which allowed the plate to move sideways during the cut. This problem was solved by improving the fixture, either by putting more weights or increasing the force used at the clamping system.

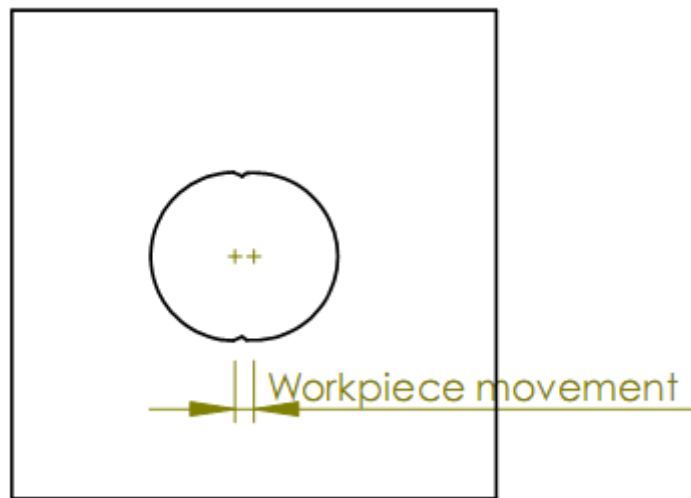


Figure 27. Schematic representation of the problems felt during the AWJC due to bad fixture.

5. CONCLUSIONS

An experimental study has been conducted in order to study, in AWJ technology, the main characteristics of the cut, which are the kerf taper angle and the kerf width and the surface quality. Since the use of the AWJ to cut layered composites, as the carbon fiber cut on this study, is growing it is important to know the effect of AWJ operating parameters on these characteristics in order to machine these materials with tight tolerances. This study aimed to learn the influence of the cutting orientation and traverse speed on the kerf taper angle, kerf width and roughness.

The cutting directions of 0, 45° and 135° showed some tendency to present greater kerf taper angles than the other directions. However this trend was not true for all traverse speeds, so some repeatability tests should be made to confirm these values.

The largest taper angle variation with the cutting orientation was obtained for the traverse speed of 2000 mm/min, with a range of values between 2.20° and 2.60°. This angle variation led to a variation of the bottom kerf width of approximately 0.03 mm, which is rather small. This effect can be of greater interest if thicker materials are cut since the bottom kerf width variation may be greater.

An increase of the traverse speed led to greater taper, which is consistent with other studies made in the field with laminate composites. The variation of the average value of taper with the traverse speed (for the range of speed from 500 to 2000 mm/min) was almost linear, which allows a correct prediction of the kerf taper for later correction with tilting techniques.

From the measured results of the kerf width, it is possible to say that the cutting orientation had no influence in this characteristic. Despite the kerf width values were only measured for $\theta = 0^\circ, 45^\circ, 90^\circ$ and 135° , since no variations were found it is believed that the kerf width for the other cutting directions would be similar. Both the top and the bottom kerf widths decreased linearly with the traverse speed. However, the decrease rate of the bottom kerf width was greater than the rate of the top kerf width change.

The cutting orientation showed the highest values of roughness for all the cut depths, at the traverse speeds of 2000, 1500 and 1000 mm/min, with exception for the

cutting angle of 22.5° that presented the highest value of roughness for a cut depth of 1 mm and a speed of 1000 mm/min. When cutting with a speed of 500 mm/min the roughness did not show to be affected by the cutting direction.

The roughness increased with the cut depth for the speeds of 2000, 1500 and 1000 mm/min, while at 500 mm/min the roughness decreased from the top to the middle and then increased again at the bottom.

The traverse rate decrease resulted in a roughness decrease, which is the same conclusion as other studies made in the field. Nevertheless the decrease rate was not linear, and different among each cut depth.

None of the tested piercing methods avoided the known defects such as delamination, fiber cracking and fiber pullout. Therefore, start cutting off the plate or drilling a start hole are preferable solutions when cutting the tested carbon fiber.

The stainless steel support slats were responsible for some defects, such as superficial scratches, frosting due to waterjet rebound on the slats, and unwanted material removal at the bottom if the exposure time to the waterjet rebound is enough. In order to avoid these problems, some cuts were made with a plate of plywood between the carbon fiber and the support slats. Although this solution eliminated the referred problems, the plywood dimensional variation due to the water absorption created other issues like stand-off distance variation along the cut and striking angle different from 90° . The low density of the plywood also increased the floating force, requiring the placement of heavier weights at the top of the set.

Although no tests were made to ascertain if delamination occurred inside the workpiece (due to the cutting process), by observation of the kerf walls at the microscope no evidences were found of delamination. Also, in most of the studies with focus on this problem, delamination started to appear at the bottom with bare-eye visible debonding of the bottom layers. No such thing was observed in any of the performed cuts, so it is believed that with the used cutting parameters it is possible to produce delamination free cuts.

Some other defects appeared during the cuts, like surface chipping, fiber partially cut at the bottom, cracking at the exit point and fiber pullout. The surface chipping showed to be directly affected by the cutting direction and traverse speed, while

the cracking at the exit point of the jet occurred with every used combination of operation parameters.

5.1. Future work guidelines

With regard to future works in the field, the following topics may prove to be of interest:

- Other sacrificial materials that do not create the same problems as plywood, due to water absorption, should be tried;
- Verify the linearity between the compensation tilting angle and the kerf taper angle in the studied material;
- Cut the studied material with a plate of sacrificial material at the entry point, since some literature in the field refer that this technique reduces the surface chipping observed in this study. References to the use of a thin aluminum plate (about 2 mm) were often found.
- Repetition tests should be made to ascertain about the influence of the cutting orientation with the kerf taper angle and the surface roughness;
- The current fixture systems are somewhat primitive. Therefore new types of fixture systems should be studied in order to allow automation of the cutting process, or at least a reduction of the time spent by the operator during the positioning of the workpiece;
- Mechanical strength tests should be made in order to acknowledge if the created defects during AWJC compromise the material performance, or are just unaesthetic.

6. REFERENCES

- Akkurt, A., Kulekci, M. K., Seker, U., Ercan, F. (2004), "Effect of feed rate on surface roughness in abrasive waterjet cutting applications", *Journal of Materials Processing Technology* 147, 389-396
- Azmir, M.A., Ahsan, A. K. (2008), "Investigation on glass/epoxy composite surfaces machined by abrasive water jet machining", *Journal of Materials Processing Technology* 198, 122-128
- B.C. MacDonald & Co. (2001), "Basic Components & Elements of Surface Topography", Last seen: 4 of June of 2011 at http://www.bcmac.com/pdf_files/surface%20finish%20101.pdf
- Boud, F., Carpenter, C., Folkes, J., Shipway, P. H. (2010), "Abrasive waterjet cutting of a titanium alloy: The influence of abrasive morphology and mechanical properties on workpiece grit embedment and cut quality", *Journal of Materials Processing Technology* 210, 2197-2205
- Cover image taken from: <http://www.lupaul.com/water.php>
- Dias, J. P. M. R. (2011), "The Effect of Velocity in Abrasive Waterjet Cutting", Master thesis in Mechanical Engineering, University of Coimbra
- Folkes, J. (2009), "Waterjet - An innovative tool for manufacturing", *Journal of Materials Processing Technology* 209, 6181-6189
- Hashish, M. (2011), "Energy Fields in Waterjet Machining", In Zhang, W. (ed), *Intelligent Energy Field Manufacturing*, CRC Press, 141-171
- Liu, H. T., Schubert, E. (2009), "Piercing in delicate materials with abrasive-waterjets", *The International Journal of Advanced Manufacturing Technology* 42, 263-279
- Mazumbar, S. K. (2002), "Composites Manufacturing: Materials, Product and Process Engineering", CRC Press
- Öjmertz, C. (2006), "A Guide to Waterjet Cutting", Water Jet Sweden AB, Ronnely
- OMAX Interactive Reference available in the waterjet machine software OMAX[®] Make and Layout both version 17
- Orbanic, H., Junkar, M. (2008), "Analysis of striation formation mechanism in abrasive water jet cutting", *Wear* 265, 821-830
- Ramulu, M., Hwang, I., Isvilanonda, V. (2009), "Quality issues associated with abrasive

-
- waterjet cutting and drilling of advanced composites”, 2009 American WJTA Conference and Expo
- Shanmugam, D. K., Masood, S. H. (2009), “An investigation on kerf characteristics in abrasive waterjet cutting of layered composites”, *Journal of Materials Processing Technology* 209, 3887-3893
- Shanmugam, D. K., Nguyen, T., Wang, J. (2008), “A study of delamination on graphite/epoxy composites in abrasive waterjet machining”, *Composites: Part A* 39, 923-929
- Shanmugam, D. K., Wang, J., Liu, H. (2008), “Minimization of kerf tapers in abrasive waterjet machining of alumina ceramics using a compensation technique”, *International Journal of Machine Tools & Manufacture* 48 (2008), 1527-1534
- Siores, E., Wong, W. C. K., Chen, L., Wager, J. G. (1996), “Enhancing Abrasive Waterjet Cutting of Ceramics by Head Oscillation Techniques”, *CIRP Annals – Manufacturing Technology* Volume 5, Issue 1, 327-330
- Wang, J. (1999), “Abrasive waterjet machining of polymer matrix composites – Cutting performance, erosive process and predictive models”, *The International Journal of Advanced Manufacturing Technology* 15, 757-768
- Waterjets.org Staff, “Waterjet brick”, Last seen on 2 of September of 2011 at http://waterjets.org/index.php?option=com_content&task=view&id=57&Itemid=54
- Zheng, H. Y., Han, Z. Z., Chen, Z. D., Chen, W. L., Yeo, S. (1996), “Quality and cost comparisons between the laser and waterjet cutting”, *Journal of Materials Processing Technology* 62, 294-298

APPENDIX A – WATERJET GLOSSARY

This chapter contains the description of some terms that are commonly used in AWJM.

Abrasive flow rate – Rate at which abrasive particles flow into the cutting nozzle.

Catch tank – Tank filled with water and placed underneath the cutting nozzle. The main function is to disperse the waterjet stream energy.

Delay time – Delay time between the introduction of abrasive particles and the jet flow start. This delay is important to avoid clogs in the mixing tube.

Jet Lag – When cutting through a material, the jet is deflected opposite to the cutting direction. This means that the jet exit point lags behind in relation to the jet entry point.

Kerf taper angle – Angle made by the kerf walls, due to different kerf width along the cut depth.

Kerf width – Distance between the created kerf walls.

Machinability – Often given as a number, it represents how easy it is for a waterjet to machine a given material.

Mixing tube – Also referred as focusing tube, it is a tube made of extremely hard material, like tungsten carbide, and is where the abrasive mixes with the water.

Nozzle – normally refer to the assembly made by the mixing tube, jewel and nozzle body

Stand-off – Distance between the surface of the workpiece and the end of the nozzle.

Support slats – part of the fixture system, they are typically stainless steel plates aligned vertically and are used to support the material when machining.

Tabbing – method for holding the workpiece fixed to the main plate, by leaving a small piece of material uncut. Useful to avoid the workpiece fall into the catch tank.

Traverse – Moving the waterjet nozzle without running water or abrasives. This movement is used to position

Traverse speed – Moving speed of the nozzle.

Waterjet brick – A rectangular piece of corrugated plastic used to avoid some problems like workpiece fall to catch tank or frosting.

APPENDIX B – CHAIN OF PROCEDURES

In this appendix it is shown the chain of procedures followed during the experimental cuts, as well as measurements made on the cut samples.

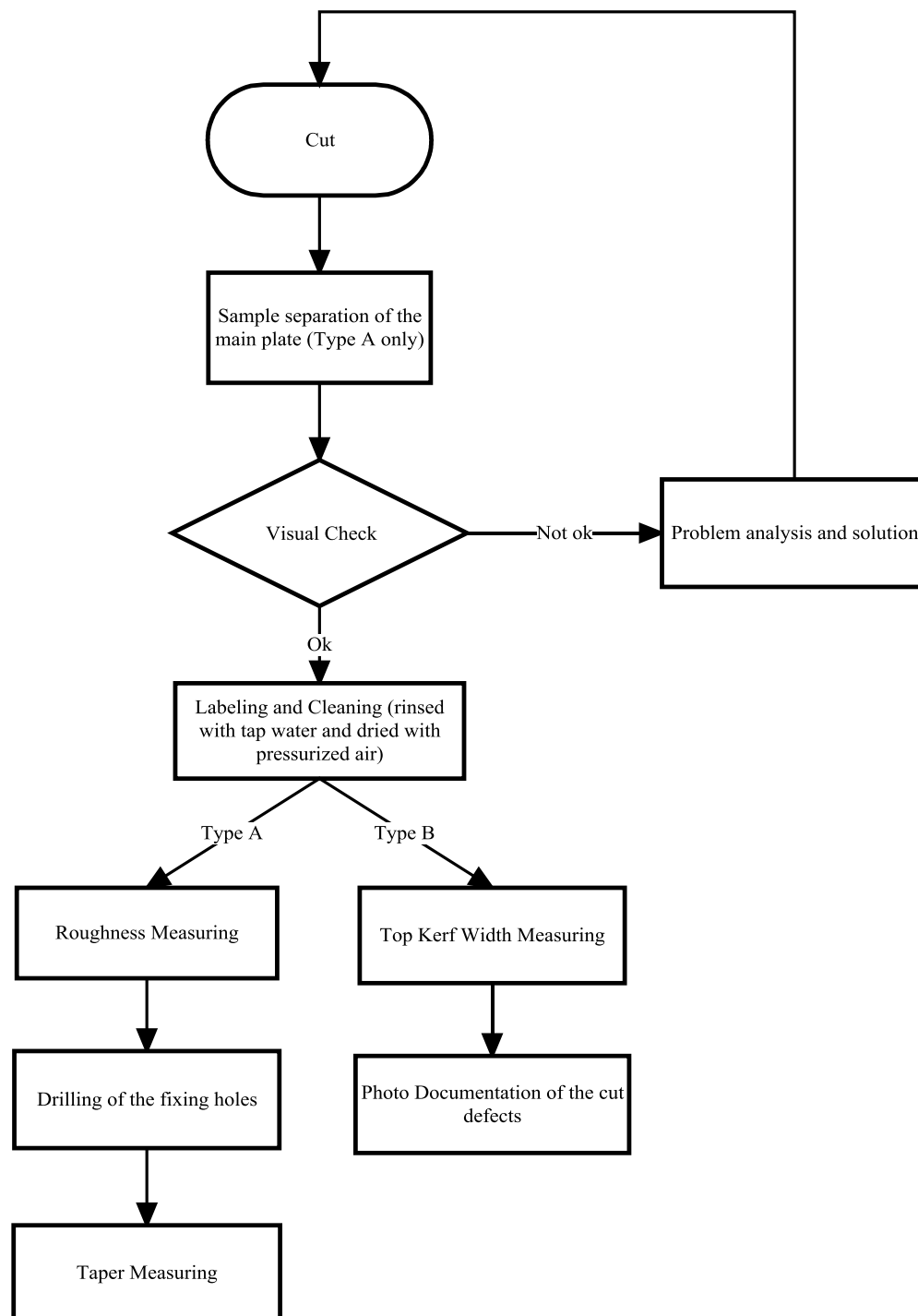


Figure 28. Chain of procedures regarding the experimental cuts and measurements.

APPENDIX C – PIERCING MEASUREMENTS

In order to ascertain which piercing methods caused greater destruction of the composite, the affected areas on the surface, both top and bottom, were measured. These areas presented an elliptical shape, as shown in Figure 29, so the A_{AP} , affected by piercing area was calculated by equation (2). The measured values and the calculated areas are shown in Table 8.

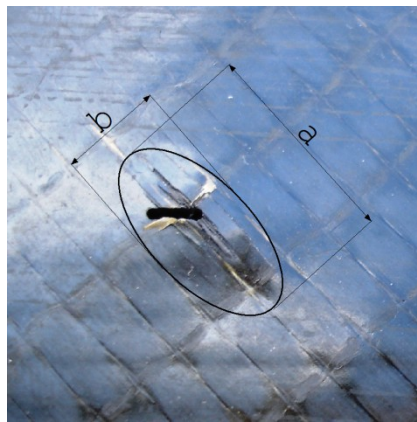


Figure 29. Schematic view of the elliptical affected area, caused by piercing.

$$A_{Ellipse} = A_{AP} = \pi \times a \times b \quad [mm^2] \quad (2)$$

, where a and b are one-half of the ellipse's major and minor axes, respectively. Both were measured in millimeters.

Table 8. Affected areas created by the tested piercing methods. L.P. stands for "Low Pressure". The piercing methods are sorted by top affected area size, low to high.

Piercing Method	Top			Bottom		
	a [mm]	b [mm]	$A_{Ellipse}$ [mm ²]	a [mm]	b [mm]	$A_{Ellipse}$ [mm ²]
L.P. Dynamic	13	7	71.5	9	5	35.3
Dynamic	16	6	75.4	8	5	31.4
H2O Only	15	10	117.8	8	6	37.7
Stationary	18	11	155.5	7	6	33.0

APPENDIX D – KERF TAPER ANGLE

The results obtained from the kerf taper angle measurements, due to its length, are shown here, in Table 9, instead of being in the chapter *Results and Discussion*.

Table 9. Measured kerf angles in degrees.

Cutting Orientation	Traverse Speed [mm/min]			
	2000	1500	1000	500
0°	2.37	2.13	1.86	1.22
22.5°	2.50	2.06	1.75	1.22
45°	2.60	2.17	1.84	1.35
67.5°	2.34	2.02	1.63	1.16
90°	2.36	2.01	1.70	1.18
112.5°	2.41	1.94	1.63	1.18
135°	2.20	2.00	1.85	1.27
157.5°	2.30	1.99	1.76	1.20
Range	0.40	0.23	0.23	0.19
Average	2.38	2.04	1.75	1.22